INSTITUT DE FRANCE
Académie des sciences

Comptes Rendus

Géoscience

Sciences de la Planète

John S. McCloy and Sophie Schuller

Vitrification of wastes: from unwanted to controlled crystallization, a review

Volume 354, Special Issue S1 (2022), p. 121-160

Published online: 28 February 2022
Issue date: 29 May 2023

https://doi.org/10.5802/crgeos.111

Part of Special Issue: Glass, an ubiquitous material
Guest editor: Daniel Neuville (Université de Paris, Institut de physique du globe de Paris, CNRS)

Les Comptes Rendus. Géoscience — Sciences de la Planète *sont membres du Centre Mersenne pour l'édition scientifique ouverte*
www.centre-mersenne.org
e-ISSN : 1778-7025

Comptes Rendus
Géoscience — Sciences de la Planète
2022, Vol. 354, Special Issue S1, p. 121-160
https://doi.org/10.5802/crgeos.111

Glass, an ubiquitous material / *Le verre, un matériau omniprésent*

Vitrification of wastes: from unwanted to controlled crystallization, a review

John S. McCloy *, [a] **and Sophie Schuller** [b]

[a] Washington State University, School of Mechanical and Materials Engineering, Pullman, WA 99164, USA

[b] CEA, DES, ISEC, DE2D, Marcoule, 30207 Bagnols-sur-Cèze, France

E-mails: john.mccloy@wsu.edu (J. S. McCloy), sophie.schuller@cea.fr (S. Schuller)

Abstract. In this review, we provide a perspective on the science and technology of vitrification of waste. First, we provide a background on the general classes of wastes for which vitrification is currently used for immobilization or is proposed, including nuclear and industrial hazardous wastes. Next, we summarize the issues surrounding solubility of waste ions and resulting uncontrolled crystallization or phase separation. Some newer waste form designs propose a controlled crystallization, resulting in a glass-ceramic. A summary of glass systems and glass-ceramic systems is given, with the focus on immobilizing waste components at high waste loading. Throughout, design and processing considerations are given, and the difference between uncontrolled undesirable and controlled desirable crystallization is offered.

Keywords. Nuclear waste, Hazardous waste, Vitrification, Glass, Glass-ceramic, Vitro-ceramic.
Published online: 28 February 2022, Issue date: 29 May 2023

1. Introduction

Vitrification is a powerful technology to immobilize nuclear [Caurant et al., 2007a, Donald, 2010, Pegg, 2015, Singh et al., 2021, Vernaz and Bruezière, 2014, Vernaz et al., 2016] and industrial [Caurant, 2017, Donald, 2007, 2010, 2016] solid and liquid wastes. Glasses and glass-ceramics (GC) have been developed worldwide since the 1970s to integrate high, intermediate, and low-activity wastes (LAW) coming from reprocessing of nuclear spent fuel, nuclear decommissioning activities, legacy radioactive waste from non-fuel cycle activities, and even industrial non-radioactive wastes. The compositions chosen have been the result of a compromise between waste loading, technological feasibility, and the physical and chemical properties of the melt and final solidified product. Alumino-borosilicate or phosphate glasses and GC are currently being developed in different laboratories, while some are already used at the industrial scale in nuclear facilities [such as La Hague (France), Hanford (USA), Savannah River (USA), West Valley (USA), Sellafield (UK), Tokai (Japan), Rokkasho-Mura (Japan), Tarapur (India), Trombay (India), Karlsruhe (Germany), and Mayak (Russian Federation)], and industrial waste treatment plants (such as the Morcenx plant, France).

* Corresponding author.

In this review, we give an overview of the major research carried out to develop glass and GC waste forms able to safely immobilize the nuclear and industrial (i.e., hazardous, non-radioactive) wastes. Emphasis is made on the nature of the waste stream, the selection of the technology, and the resulting phases in the waste form. Since many waste elements of importance have low solubility in typical oxide glasses, sequestering them into crystalline phases in GCs is an increasingly used strategy for immobilization.

2. Background

2.1. *Industrial wastes*

A large number of hazardous wastes, coming from industry, can be immobilized by vitrification for storage or for reuse in some other technology. These wastes are formed by different processes, such as incineration of household waste, lagoon sludges, coal-fired power plants (coal fly ash), ferronickel smelting (slag and dust), or infrastructure dismantling [Caurant, 2017]. The particularity of this type of waste is normally its high quantity of glass formers and modifiers (e.g., SiO_2, CaO). This characteristic gives the advantage that glass or GC can be formed at high temperature with little to no addition of additional glass-forming precursors (Table 1). Research on glass fibers [Ma et al., 2018, Scarinci et al., 2000] and GCs [Karamanov et al., 2017, Ljatifi et al., 2015, Rawlings et al., 2006] by vitrification of waste are underway to find the viability, through lower cost and good physical–chemical properties, which will enable commercial applications. Asbestos vitrification, for instance, is now a powerful process to destroy the asbestos fiber structure, transforming it into an asbestos-free and vitrified end product [Spasiano and Pirozzi, 2017]. In general, reported science in the area of vitrification is still in its infancy compared to nuclear waste processing, which will constitute the bulk of this review.

2.2. *Nuclear wastes and technologies*

Nuclear wastes management is a major worldwide challenge. Its implementation depends on the strategy, economy, and policy of individual countries; however, in most of them, glass and GC matrices are used to immobilize the nuclear wastes coming from the reprocessing of spent fuel, legacy waste such as from weapons manufacturing, or dismantling and decommissioning of nuclear facilities. Radioactive waste classification and hence waste management does differ from country to country, however the general strategy adopted internationally for High-activity Level Waste (HLW) is high temperature vitrification, or the formation of glass from the waste plus additives [Lee et al., 2013].

The type of nuclear wastes coming from reprocessing of spent fuel [Glatz, 2020] burned in different power reactor technologies [Hayward, 1988b]—e.g., PWR – *Pressurized Water Reactor*, BWR – *Boiling Water Reactor*, PHWR – *Pressurized Heavy Water Reactor* (CANDU – Canada Deuterium Uranium), GCR – *Gas-Cooled Reactor* (NUGG – *Natural Uranium Graphite Gas reactor*, Magnox, AGR – *Advanced Gas-cooled Reactor*), AHWR – *Advanced Heavy Water Reactor*, RBMK – *Reaktor Bolshoy Moshchnosti Kanalnyy* = advanced graphite-moderated nuclear power reactor—is given in Table 2. It is likely that new reactor types (e.g., molten salt reactors, high temperature gas reactors) will require new and different waste forms, which may or may not be vitrified.

Several aspects influence the waste stream. For instance, the cladding materials vary considerably and can have an important effect in waste chemistry (e.g., Mg alloy in Magnox, steel in UK Advanced Gas Reactor, Zr alloy in most others, Al at Hanford non-power reactor). Additionally, the form of the U fuel, enrichment, and burnup will influence the amount and nature of the fission products. Finally, the chemical separations used for any reprocessing, as well as secondary chemical reactions occurring during storage (e.g., corrosion of storage tanks, aging of fuel in cooling ponds) will add further to the waste coming to the beginning of the vitrification process. In some cases, where used fuel is relatively constant in character, a single glass composition can be characterized and used repeatedly, such as the R7T7 borosilicate glass developed by CEA (Commissariat à L'Énergie Atomique et aux Énergies Alternatives) and the French commercial waste processing company Orano (formerly Areva).

These wastes are processed using the five main vitrification technologies (Table 3)—Joule-Heated Ceramic Melter (JHCM), Cold Crucible Induction Melter (CCIM), Hot Crucible Induction Melter (HCIM), indirect heating using a metallic susceptor,

Table 1. Summary of some industrial waste types, compositions, vitrification processes, and level of commercialization

Type of industrial wastes	Process	Vitreous precursors	Type of wastes	Nuclear plant	Countries	Ref
Municipal incinerator of Reggio Emilia, Italy, and sludge excavated from the lagoon of Venice	Recycling glass fiber—lab scale 1400 °C	SiO_2, Al_2O_3, CaO, MgO, Na_2O, K_2O	SiO_2, Al_2O_3, CaO, MgO, Na_2O, K_2O, BaO, B_2O_3, ZrO_2, PbO, TiO_2, Fe_2O_3, Cr_2O_3, ZnO, SO_3, SrO, P_2O_5, MnO	No industrialization to date	Italy	Scarinci et al. [2000]
Coal fly ash coming from coal-fired power plants	Recycling glass fiber 1300–1350 °C—lab scale	SiO_2, MgO, CaO	SiO_2, Al_2O_3, CaO, Fe_2O_3, other metals (As, Be, B, Cd, Cr, Co, Pd, Mn, Hg, Se, Sr, V)	No industrialization to date	China	Ma et al. [2018]
Slag and dust coming from ferronickel smelting	GC synthesis 1400 °C—lab scale	SiO_2, MgO, CaO, Al_2O_3, Na_2O, K_2O	SiO_2, Al_2O_3, MgO, CaO, Cr_2O_3, CoO, NiO, Fe_2O_3	No industrialization to date	Bulgaria	Karamanov et al. [2017], Ljatifi et al. [2015]
Asbestos from dismantling	Vitrification of asbestos 1400 °C–1500 °C	—	Minerals SiO_2, MgO, CaO	• Morcenx plant (France) since 1999—Inertam Europlasma since 2020 • GeoMelt® treatment plant in Japan • Neutramiante SAS	France UK/Japan US	Spasiano and Pirozzi [2017]
Tailings and fly ash from rare earth mine	GC synthesis 1450 °C—lab scale	Na_2O, K_2O	SiO_2, MgO, CaO, Al_2O_3, Fe_2O_3, rare earth oxide	No industrialization to date	China	Chen et al. [2019a]

"Vitreous precursors" implies the components forming the basis of the glass. These are not necessarily added, as can be seen from the composition of the waste oxides "types of waste".

Table 2. Some properties of reactors and the fuel configuration influencing the nuclear waste, after Hayward [1988b]

	Magnox	NUGG	AGR	Candu	PWR	BWR	RBMK	Hanford
Country of origin	UK	France	UK	Canada	US	US	USSR (Russia)	US
Fuel	U metal rod	U–Mo metal	Oxide pellets	Oxide pellets	Oxide pellets	Oxide pellets	Oxide pellets	U metal rod
^{235}U content	Natural U (0.7%)	Natural U (0.7%)	2–3%	Natural U (0.7%)	2–4%	2–4%	2%	Natural U (0.7%)
Fuel cladding	Mg alloy	Mg–Zr alloy	Stainless steel	Zr alloy	Zr alloy	Zr alloy	Zr–Nb alloy	Al alloy
Moderator	Graphite	Graphite	Graphite	D_2O	H_2O	H_2O	Graphite	Graphite
Coolant	CO_2	CO_2	CO_2	D_2O	H_2O	H_2O	H_2O	H_2O

and In-Can Melter—adopted by the United States (US), France, Japan, India, Russia, and the United Kingdom (UK) to immobilize nuclear wastes. The specificities of these technologies are given in various publications [Goel et al., 2019, Harrison, 2014, Kaushik, 2014, Pegg, 2015, Raj et al., 2006, Short, 2014, Vienna, 2010, Walling et al., 2021a,b]. The common objective is to optimize the immobilization of nuclear waste in a glass or GC matrix. The direct feeding of nuclear waste solutions in the crucible has been chosen by almost all countries, except France and the UK. A two-step process of calcination–vitrification is used in La Hague (France) and Sellafield (UK) facilities. In all cases, glass precursors (beads, glass frit, mixed additives as solid or liquid) and nuclear wastes (calcine, solution, and/or sludge) are fed into the crucible and then heated at the synthesis temperature. After sufficient melting and homogenization, the molten glass is poured into steel containers (except for the case of In-Can Melter technology). The challenge, in all cases, is to take into account the specificity of the waste stream, while optimizing technology, process, and the properties of the resulting host glass or GC matrices.

3. Glass waste forms

In the vitrification technologies field, the best compromise must be obtained among specification of wastes and final glass, glass and melt properties, and the vitrification process and resulting costs. This tricky balance of properties, processing, and cost requires tremendous amounts of knowledge as well as ongoing research and development. In this section, we describe the key parameters and key properties involved in glass waste form development.

In the case of glass or GC waste form matrices developed for the vitrification of industrial and nuclear wastes, the chemical–physical properties of four states of glass during production—glass batch, glass melt, undercooled melt, solid glass—have to be managed along with the vitrification processes connecting these states (glass-batch heating, glass melting and refining, cooling and storage) as shown schematically in Figure 1.

3.1. *Waste incorporation in glasses*

Due to their amorphous state and their structural disorder, one of the specific characteristics of oxide glasses and GCs is their capacity to contain a wide variety of chemical elements belonging to all groups of the periodic table. The integration of cations in the vitreous network depends on the intrinsic nature of the atoms (ionic radius and charge), their synergistic effects (glass composition and former or modifier type structural roles within the vitreous network), and the glass synthesis conditions (temperature, reaction time, gaseous atmosphere). Many publications give information about the structural role of different cations coming from hazardous elements or nuclear wastes in a simplified borosilicate network [Caurant et al., 2009, Caurant and Majérus, 2021, Donald, 2010].

A useful correlation between the oxidation state and the conditional chemical solubility of elements in alumino-borosilicate glass has been suggested recently [Gin et al., 2017] (Figure 2). It indicates that in the case of cationic species, the conditional solubility of cations decreases proportionally with the increase in the oxidation state. Therefore, elements such as Mo^{6+}, $Tc^{4+/7+}$ [Jin et al., 2015, Soderquist et al., 2014],

Table 3. Summary of vitrification processes and their realization industrially

Type of wastes spent fuel	Process	Vitreous precursors	Type of wastes	Industrial Nuclear plant	Countries	References
Military Pu spent fuel	JHCM (Joule-Heated Ceramic Melter)	Liquid feed mixed with glass additive and raw minerals		WVDP (West Valley Demonstration Project) New York (1995–2003)	US (DOE—Department of Energy)	Goel et al. [2019], Vienna [2010]
• Effluent Fe, Al • Effluent Na • Effluent enriched in halogen (SO_3, Cl, F) + Cr • Effluent enriched in Al • Effluent enriched in P, Bi, Th, Zr	1150 °C	*Hematite* (Fe_2O_3), *Borax* ($Na_2B_4O_7{\cdot}10H_2O$), *Wollastonite* ($CaSiO_3$), *Kyanite* (Al_2SiO_5), *Zircon* ($ZrSiO_4$)		DWPF (Defense Waste Processing Facility) Savannah River, SC (1996–present) WTP (Waste Treatment & Immobilization Plant) Hanford, WA		
• Magnox spent fuel (Mg, Al) • Blend spent fuel Magnox-POCO (Post Operational Clean Out), Mo	Calcination vitrification HCM (Hot crucible Melter)	Solid	Solid	WVP (Waste Vitrification Plant) Sellafield 1990–present	UK (BNFL—British Nuclear Fuels Limited)	Harrison [2014], Short [2014]
	1050 °C	Glass frit sodium alumino-borosilicate	Calcine			
• Natural U HLW—PHWR (Pressurized Heavy Water Reactor) Spent fuel	First generation indirect heating using a metallic susceptor			WIP (Waste Immobilization Plant) Tarapur	India (BARC—Bhabha Atomic Research Centre)	
• U/Th HLW—AHWR (Advanced Heavy Water Reactor) spent fuel • Th, U, Al, F, Fe, Ni, Cr Spent fuel UOX spent fuel (PWR) • UOX spent fuel (Boiling Water Reactor) • HLW + SO_3, U, Na	Second generation JHCM (Joule-Heated Ceramic Melter) 1000 °C–1050 °C	Liquid	Liquid	WIP (Waste Immobilization Plant) Trombay		Kaushik [2014], Raj et al. [2006]

(continued on next page)

Table 3. (continued)

Type of wastes spent fuel	Process	Vitreous precursors	Type of wastes	Industrial Nuclear plant	Countries	References
• UOX spent fuel • BWR spent fuel	JHCM (Joule-Heated Ceramic Melter) liquid-fed ceramic melter	Solid Glass bead sodium alumino-borosilicate	Liquid	Rokkasho-Mura (2006–present) Tokai (1994–2017)	Japan (JNFL—Japan Nuclear Fuel Limited)	Okubo [2018], Yoshioka et al. [1992]
• UOX spent fuel • UMo spent fuel	Calcination–vitrification HCM (Hot crucible Melter) 1100 °C and CCIM (1200 °C–1250°C)	Glass frit sodium alumino-borosilicate	Calcine	La Hague (R7/T7) (1992–present)	France (ORANO)	Vernaz and Bruezière [2014], Vernaz et al. [2016]
• HLW nuclear legacy wastes: VVER-440, Fast, Neutron reactors BN-600, nuclear navy, research reactors, spent fuel	JHCM (Joule-Heated Ceramic Melter) liquid-fed ceramic melter In 2015 there will start operation of a new vitrification installation EP-500/5 instead of the expired EP-500/4. The technology is experimental on the use of the induction melter "cold crucible" that will vitrify accumulated HLW with complex composition.	Solid Glass frit alu-minophos-phate	Liquid	**Mayak** (**1986–2015** EP-500/4.) (**2015–present** EP-500/5)	Russian Federation	[Nucelar Energy Agency (NEA), 2014; Stefanovsky et al., 2019, 2016]
• Fukushima waste Zeolite; Cs, Sr	In-can melter/Cold crucible 1000–1100 °C	Glass frit	Solid	**Under industrialization**	France, Japan, UK, Korea	[Didierlaurent et al., 2019, 2020, Kimura et al., 2018, Oniki et al., 2020]

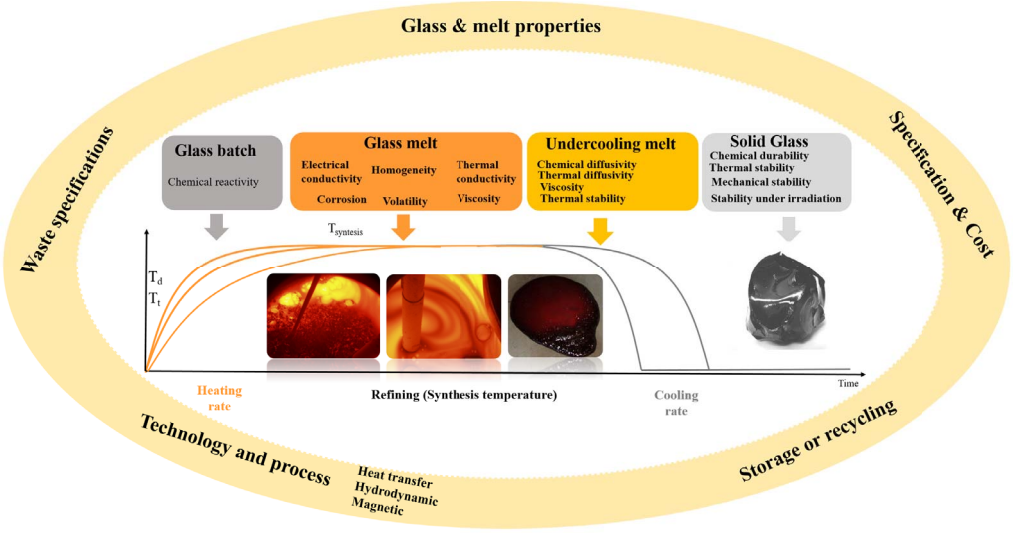

Figure 1. Illustration of cyclical optimization of glass and melt properties, technology, storage, specifications of wastes, and final glass, as related to the different steps of vitrification and glass states.

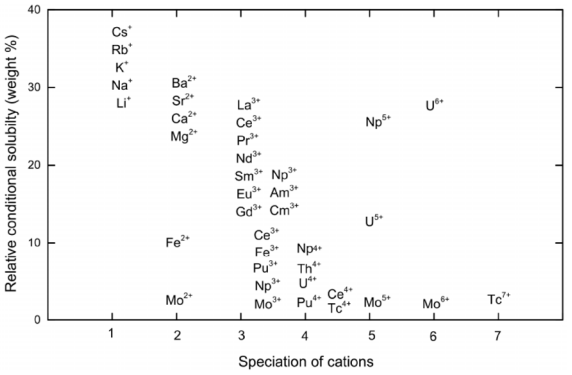

Figure 2. Conditional solubility of elements related to their cation speciation in the aluminoborosilicate glasses—after Gin et al. [2017].

S^{6+} [Lenoir et al., 2009, Manara et al., 2007], Ce^{4+}, and actinides (Pu^{4+}, U^{4+}, Th^{4+}, Np^{4+}, Am^{3+}, Cm^{3+}) [Deschanels et al., 2003, Lopez et al., 2003, 2005] have very low solubility compared to alkali and alkaline-earth metals. One should note that this schema does not hold for reduced metals Ru^0, Pd^0, Rh^0, Ag^0, Mo^0 or anionic species Cl^-, I^- [McKeown et al., 2015, Muller et al., 2014, Riley et al., 2014] that also present very low solubility in oxide glass. These elements can have a large impact on glass waste form optimization.

Taking into account the composition of the waste and the solubility of species in the glass, waste loading is optimized to obtain a homogeneous amorphous matrix or an amorphous matrix containing some crystalline phases. A wide range of crystalline phase assemblages in term of nature, size and morphology can be formed at melt temperatures or during cooling (see Figure 3). The challenge remains to control their formation and their impact on the vitrification process and resulting waste form properties.

3.2. *Matters of terminology*

In GCs, narrowly defined [Deubener et al., 2018], the material is processed as a glass and one or more crystalline phases is precipitated under *controlled* heat treatment. The final product has both "residual" glass along with ceramic phases. Several previous summaries have expounded upon GCs for waste applications [Caurant, 2017, Caurant et al., 2009, Donald, 2010, McCloy and Goel, 2017]. The ceramic phases are designed to accommodate in their crystal structure one or more of the radionuclides or other waste products.

Some authors have used glass composite materials (GCMs) to denote all forms of crystals in glass fabricated deliberately, including those materials where a glass binder frit encapsulates and consolidates previously synthesized ceramic waste crystals

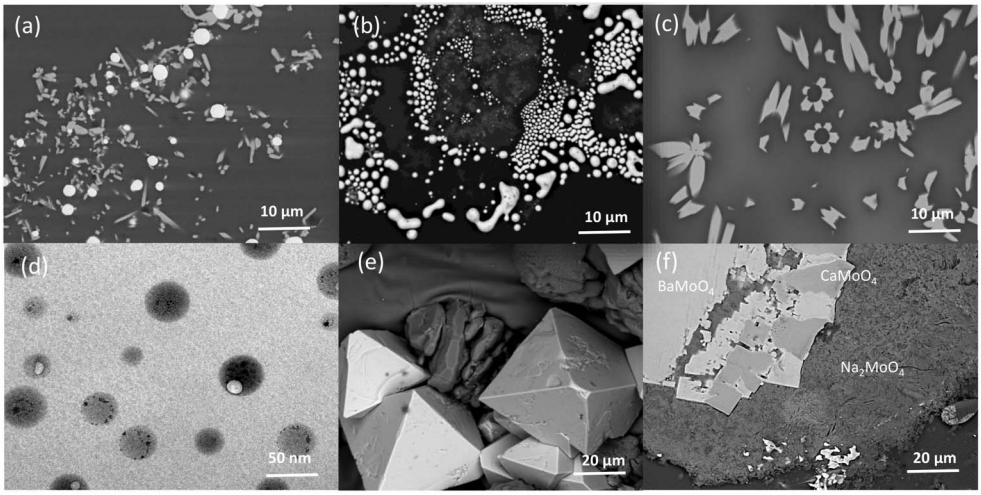

Figure 3. Crystals and separated phases in simplified borosilicate nuclear glasses obtained after heating and cooling (a) RuO_2 needles and spherical Pd–Te; (b) agglomeration of Pd–Te; (c) $Ca_2Nd_8(SiO_4)_6O_2$ crystals; (d) nano-separated phases enriched in MoO_3 and Na_2O; (e) $CaMoO_4$ embedded in a separated phase; (f) simplified yellow phase assemblage (Na_2MoO_4, $CaMoO_4$, $BaMoO_4$).

[Lee et al., 2006, McCloy and Goel, 2017, Ojovan et al., 2021]. A wide variety of processing methodologies and their important parameters for glass composites are discussed elsewhere [Donald, 2010, Ojovan et al., 2008].

Other authors have classed these glass binder + ceramic systems as GCs [Caurant, 2017, McCloy and Goel, 2017], though these are contrasted with "real" GCs which have *induced* crystallization [Deubener et al., 2018]. Further, it is our understanding that the French term vitro-céramiques, as used within the commercial glass industry, is strictly for glasses processed by nucleation and growth. Finally, the term "spontaneously crystallized glass-crystalline material" has been used to indicate *uncontrolled* devitrification, translated as "mineral-like materials" in the Russian literature and "glassy slags" in some English literature [Stefanovky et al., 2004].

In this review, we restrict ourselves to a discussion of *uncontrolled* crystallization and the problems it causes (Section 3.3), as well as *controlled* crystallization, whether by cooling a melt or heating, then cooling glass (Section 4).

3.3. *Unwanted crystals in nuclear waste glasses*

While controlled crystallization can be used to increase waste loading in glasses, uncontrolled crystallization can result in both processing problems and waste form performance issues, particularly losses in chemical durability [Hrma, 2010]. Additionally, the failure of crystalline materials from the batch to adequately dissolve or react in an uncontrolled way can cause both processing challenges and undesirable intermediate liquid phases.

3.3.1. *Yellow phase*

During batch-to-glass conversion, one of the main issues of HLW vitrification wastes coming from reprocessing of uranium oxide (UOX) spent fuel is the formation of the "yellow phase" (alkali and alkali-earth molybdate phases, usually colored yellow due to small amounts of chromate). This phase is observed in liquid feed or solid feed processes, limiting the amount of high-level radioactive waste loading in glass. Up to the incorporation rate of MoO_3 (about 1 mol%), yellow phase can be formed by a phase separation of molten salts from the borosilicate melt, and this molybdate salt phase crystallizes separately from the borosilicate glass during cooling in the canister. The composition of the initial glass and waste have a high impact on crystalline phase assemblage of the yellow phase. Its composition is able to incorporate significant amounts of alkali—Na [Boué et al., 2019], Li [Rose et al., 2011],

Cs [Kroeker et al., 2016]—and alkali-earth (Ca, Ba) metals as well as other minor elements such as rare earth metals, Re/Tc, S, P [Usami et al., 2013] and Cr. The formation of this salt phase must be avoided because it leads to the corrosion of the processing crucibles and can alter the long-term glass performance. Consequently, much research has been conducted on this subject to find the best solution to avoid yellow phase formation [Pegg et al., 2010], but no industrial solution has yet been implemented.

However, recent fundamental research has opened perspectives on this topic. In one approach, the glass composition is altered to increase the Mo solubility. The important role of rare earth metals (Nd, La, Sm, Yb, Er) [Brehault et al., 2018, Chouard et al., 2016, Patil et al., 2018] to increase the solubility of MoO_3 in borosilicate glass and decrease the phase separation and eventual crystallization of alkali molybdate has been reported. The role of Nd is specifically explained, in sodium aluminoborosilicate enriched in MoO_3 and Nd_2O_3, by the dispersion of MoO_4^{2-} units in the borate network stabilized by Nd^{3+}, (Nd–Mo–B–O) [Brehault et al., 2018]. Without Mo present, increasing amounts of Nd result in clustering in a borate phase that separates from silicate in borosilicate glasses [Kamat et al., 2021], an effect which can be seen in crystallization behavior as well [Chen et al., 2020]. The formation of alkaline-earth molybdate phases like powellite is discussed later in this review in the context of GCs.

Another approach to controlling yellow phase formation was reported in a recent study carried out to support the Japanese liquid-fed ceramic melter technology (Figure 4). Here it has been shown how a fine grain size of the glass precursor (i.e., frit) can increase the chemical reactivity between liquid waste and glass and decrease the yellow phase formation [Uruga et al., 2020]. Results show that the incorporation rate of $NaNO_3$ (originally in the liquid waste) into the feed glass in the reactive zone (cold cap) increases as the glass grain size decreases, in a range of 2 mm (beads) to <68 μm (glass powder). In this manner, the rapid dissolution of $NaNO_3$ into the glass powder inhibited liquid Na_2MoO_4 that otherwise formed originally by reaction with MoO_3. This mechanism is probably able to limit the formation of solid water-soluble alkali molybdates, especially when combined with glass chemistry approaches using alkaline-earth and/or rare earth elements additions.

3.3.2. *Sulfate*

In some US, Indian, and Chinese wastes, high sulfur contents combined with high alkali can result in the formation of similar "yellow phase" type salt phases where sulfate SO_4^{2-} takes the role of molybdate [Billings and Fox, 2010, Lei et al., 2021, Mishra et al., 2008, Sengupta et al., 2013]. Work is ongoing to understand the glass compositional effects of sulfate salt formation [Bingham et al., 2017, Kruger et al., 2010, Skidmore et al., 2019], its relation to solubility [Vienna et al., 2004, 2014], and its structural role in the glass [McKeown et al., 2001, 2004, Xu et al., 2021]. There are many similarities between the tendency for salt phase formation with molybdate, sulfate, and other oxyanions like those of Re and Tc [Riley et al., 2013, Soderquist et al., 2016].

Due to the very low solubility [Vienna et al., 2014] in alumino-borosilicate and its propensity to volatilize, sulfates are also a major issue for the LAW vitrification. Many studies have been dedicated to the optimization of the glass composition [Kaushik et al., 2006] in order to increase the waste loading. Based on large number of data, a statistical model applicable to current US LAW glasses from the Hanford site has been applied for many glass components. A complementary approach has been to rationalize a linear relationship between retained sulfate (SO_4^{2-}/mol%) with the total cation field strength index, $\Sigma(z/a^2)$, the optical basicity, Λ^{th}, and the non-bridging oxygens per tetrahedron ratio, NBO/T [Bingham et al., 2017]. This predictive tool offers promising prospects to optimize new glass compositions with higher sulfate capacities.

3.3.3. *Spinel*

Other crystals can form in nuclear waste glasses, which may or may not be detrimental to the final waste form. For instance, spinel crystals (Figure 5a) can form at the liquidus temperature in glasses made from legacy defense wastes when melted in a Joule-Heated Ceramic Melter (JHCM). These crystals form due to saturation of transition metals in the waste or through interaction with the Cr-containing ceramic refractory [Jantzen et al., 2015]. Spinel crystals have a compositions AB_2O_4, and depending on the initial composition of the waste (e.g., A = Mn, Fe, Co, Ni, Zn and B = Fe, Cr), these have variable liquidus temperatures (950–1100 °C)

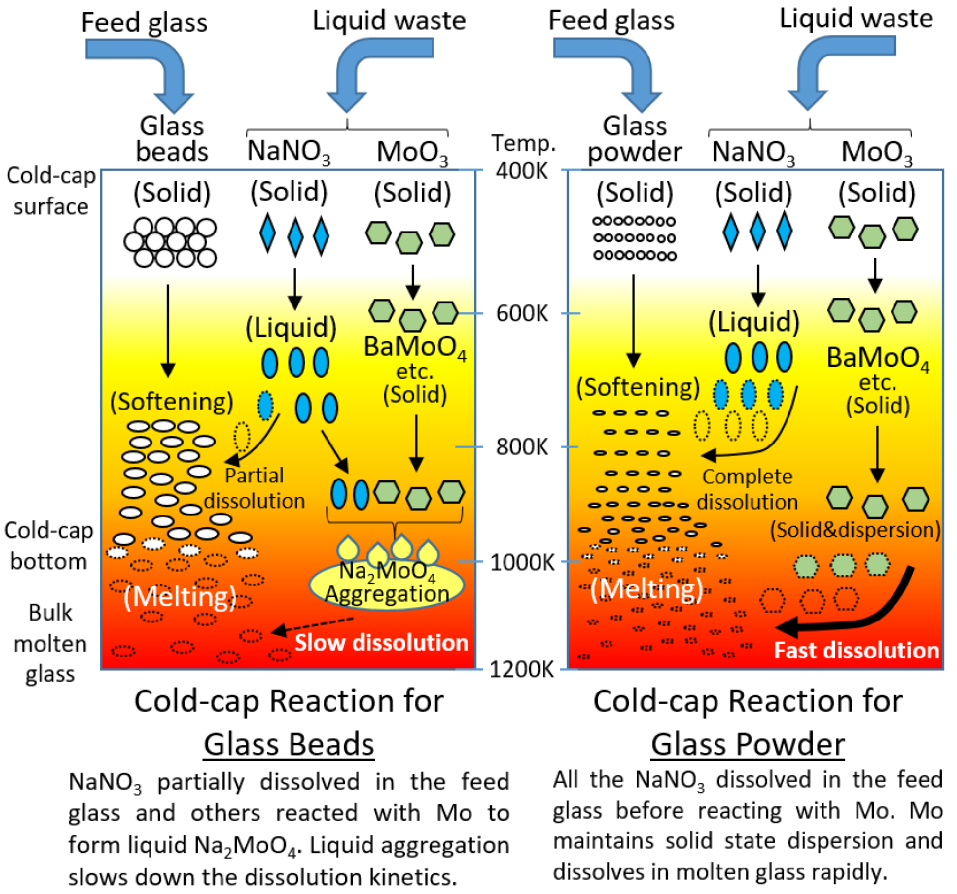

Figure 4. Cold-cap reaction model to explain the inhibition of Na_2MoO_4 formation with rapid dissolution of $NaNO_3$ into fine grain size glass powder. From Uruga et al. [2020], copyright Taylor and Francis, used with permission.

[Hrma et al., 2014, Matyáš et al., 2017]. Spinel crystals do not affect glass durability; however, they can impact the rheological behavior of the melt [Míka et al., 2002] and if accumulated in the bottom, they can block the discharge of molten glass into canisters [Guillen et al., 2019]. To avoid these phenomena, waste loading is limited to obtain a reasonable amount of spinel and low liquidus temperature.

A large panel of studies has been dedicated to the mechanism of spinel crystallization and models have been built to predict their formation [Jantzen and Brown, 2007] and dissolution [McClane et al., 2018]. A large number of publications and important results have been reported in the literature concerning the glass-batch conversion in the cold cap for Hanford vitrification technology (Waste Treatment and Immobilization Plant) [Goel et al., 2019]. This is important since the mechanism of spinel crystallization was explained by the formation of a primary spinel phase in the cold cap and then by their partial dissolution [Izak et al., 2001]. The remaining spinel phases act as nuclei for secondary spinel growth in the melt above the liquidus temperature. Empirical kinetic models based on KJMA (Kolmogorov–Mehl–Johnson–Avrami) [Casler and Hrma, 1999] and Hixson–Crowell [Hixson and Crowell, 1931] have been developed to quantify spinel dissolution and growth [Alton et al., 2002a,b, Hrma, 2010]. Supported by liquidus temperature models [Hrma et al., 2014, Vienna et al., 2001] and by predictive modeling of crystal accumulation in the glass melter [Matyáš et al., 2017], the potentially deleterious consequences of spinel crystallization can be accurately controlled.

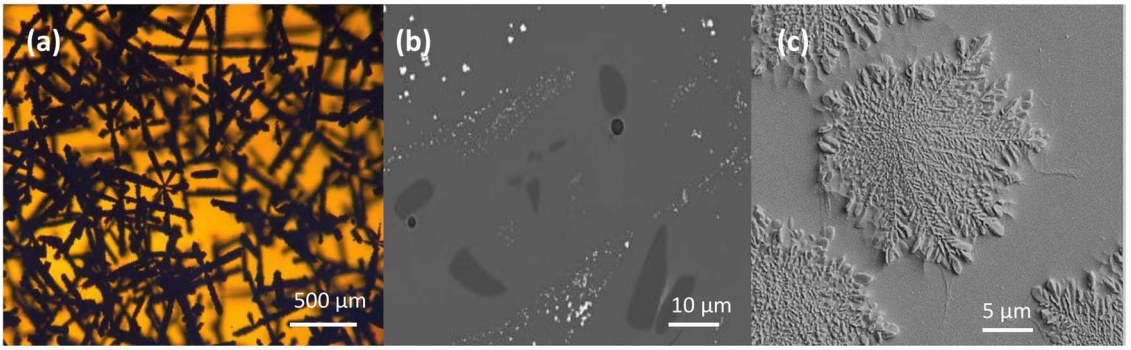

Figure 5. Examples of undesirable crystalline phases formed during vitrification process. (a) Transmitted-light optical image of spinel dendrites for Ni1.5/Al10 glass heat treated at 850 °C for 7 days, from Matyáš et al. [2017], copyright Elsevier, used with permission; (b) scanning electron micrograph showing quartz residues (dark gray) and spinel crystals (white) in glass under the cold cap, from Pokorny et al. [2013], copyright Elsevier, used with permission; (c) surface crystallization of nepheline dendrites, from Lu et al. [2021], copyright Elsevier, used with permission.

3.3.4. *Quartz*

A similar approach has been developed to manage the dissolution of quartz (SiO_2) that can remain undissolved from batch-to-glass conversion and into the melt (Figure 5b). In some nuclear waste vitrification scenarios, such as that at Savannah River Site (SRS, USA), SiO_2 glass former is added as a frit with other materials like B_2O_3. At other sites, like Hanford (USA), SiO_2 is added as an individual glass-forming chemical additive. The main reason for the difference is the wider range of waste types at Hanford, and the plant operation protocol. At SRS, a glass frit is formulated for a particular "sludge batch" of waste, and then used in the melter for many months. By contrast, at Hanford the plant is designed to quickly respond to the large variation in waste composition by using glass-forming chemicals, which are mixed in a slurry with the waste feed prior to being charged into the melter [Vienna et al., 2006].

As SiO_2 is the major glass former in borosilicate glasses, this issue is critical, as it impacts the melt rate and therefore overall cycle time. Due to the high liquidus temperature, dissolution of silica sand is generally the slowest process during glass-batch melting. One of the challenges is to control the dissolution process and identify the best conditions able to decrease the undissolved quartz fraction in the glass-forming melt. The major solution reported in the literature is the optimization of the sand grain size added to the waste. Fine grain sizes dissolve faster than larger ones in the cold cap and also affect the cold-cap physical properties (viscosity, volume fraction of bubbles, density and thermal conductivity), and these small quartz grains also improve the homogeneity of the melt [Schweiger et al., 2010, Sheckler and Dinger, 1990]. Kinetic models have been developed to describe dissolution of quartz particles in simplified glass-batch (regular particle-size distribution) [Hrma et al., 2011] and real batch (irregular shape) [Hrma and Marcial, 2011, Pokorny et al., 2013]. The kinetic equations based on relationships between quartz fraction and heating rate are currently coupled [Ueda et al., 2021] in the three-dimensional mathematical modeling of the batch-to-glass conversion developed for JHCM. In such a model, reaction kinetics are coupled with a heat transfer model in the glass batch, which considers temperature-dependent effective heat capacity, heat conductivity, and density [Goel et al., 2019].

3.3.5. *Nepheline*

For some US defense HLW where high aluminum concentration results from the dissolution of Al-clad fuel, an additional undesirable crystalline phase can form. During the step of cooling of the melt inside the canister, the sodium aluminosilicate mineral nepheline ($NaAlSiO_4$) can form (Figure 5c), removing Si and Al from the residual vitreous matrix, resulting in a deleterious impact on the glass durability [Li et al., 1997, McCloy and Vienna, 2010]. Consequently,

discriminator factors have been determined to assess compositions that suppress nepheline formation [Goel et al., 2019, Sargin et al., 2020]. But simple compositional constraints result in overly conservative formulation approaches which limit waste loading of high aluminum wastes, and thus a great deal of research has been carried out to define alternative nepheline management approaches (e.g., new glass compositions, processing conditions). Studies are mostly dedicated to determining the correlation between crystallization of nepheline and compositional domains [McCloy et al., 2011] and crystallization mechanisms [McClane et al., 2019] or post-crystallization glass structures [McClane et al., 2021], in order to develop predictive modeling. The addition of a high concentration of B_2O_3 in the glass batch has been consistently observed to reduce the propensity of nepheline crystallization by reducing the concentration of Na_2O in the melt, and thus preventing reactions with alumina tetrahedra needed to nucleate nepheline [Deshkar et al., 2020, Fox et al., 2008, Li et al., 2003]. Most recently, glass structural descriptors have been indicated to affect nepheline crystallization, particularly when affecting the local environment required for nepheline crystallization. Specifically, arrangement and coordination of Na atoms [Marcial and McCloy, 2019, Marcial et al., 2019] in the glass relative to the crystalline phase affects the likelihood of crystallization. Additionally, the presence of other framework cations like boron [Deshkar et al., 2020, Krishnamurthy et al., 2021] and phosphorus [Lu et al., 2021] in the glass break a number of Si–O–Al bonds needed for nepheline formation, rather forming significant numbers of Si–O–B or Al–O–P bonds, respectively. However, there still appear to be some exceptions to the action of B_2O_3 or P_2O_5 on nepheline crystallization. When there is a high concentration of non-bridging oxygens and glass network unmixing, as there may still be the possibility of Na–Al–Si regions concentrated and unconnected to the borate network [McCloy et al., 2015]. Similarly for P_2O_5 in high concentrations in glass, heat treatment induces phase separation and crystallization of Na_3PO_4 which in turn nucleates nepheline [Li et al., 2021].

3.4. *Additional processing considerations*

Another important issue is the volatility of elements during glass melting and refining. Volatility can modify the glass composition and have an impact on off-gas treatment and processing. Volatilization from glass melts is usually described by a combination of diffusion/evaporation processes, such as diffusion of the volatile species through the melt toward the surface, evaporation of the volatile species from the surface, and diffusion of the volatile species through the gaseous phase. Moreover, the mechanism occurs mainly through the formation of a molten salt in the cold cap and by its subsequent volatilization. These phenomena have been specifically observed for Cs [Parkinson et al., 2007] and Re/Tc in LAW. Recent reviews [Kim and Kruger, 2018, Xu et al., 2015b] have reported that molten alkali (Li, K, Na, Cs) pertechnetate(liquid) or perrhenate(liquid) usually forms in the cold cap before its volatilization at the glass surface, instead of decomposition into alkali oxides and Tc_2O_7 or Re_2O_7. Another recent study proposes an effective means to manage this volatility in the off-gas waste stream by added spinel-forming minerals (e.g., Ni-doped $Fe(OH)_2$) that can simultaneously reduce ^{99}Tc(VII) to ^{99}Tc(IV) and incorporate reduced ^{99}Tc(IV) into the stable spinel minerals [Lukens et al., 2016, Luksic et al., 2015, Wang et al., 2019].

As stated previously in the context of quartz (Section 3.3.4) and in general terms (Section 2.2), there are different approaches to feeding waste plus glass formers into the melter. Waste can be calcined or liquid, alone or mixed with glass-forming chemicals. Additives can be introduced to the waste as chemical or mineral precursors or as glass frit. The different choices depend on multiple factors associated with the process flow [Kruger et al., 2013]. For instance, in some cases it may be quite useful to be able to make small adjustments to the added chemicals depending on a given waste, especially in a continuous process, and this is facilitated by adding the glass-forming and modifying chemicals directly to a liquid feed, as is done at Hanford [Vienna et al., 2006]. Since at Hanford the waste is separated, different formulations can be used for the Hanford high-level waste (HLW) and the LAW which have different compositional profiles. For LAW, for example, additions of minerals containing particular metals of interest are used which also contain SiO_2 for glass forming, such as wollastonite ($CaSiO_3$), kyanite (Al_2SiO_5), and zircon ($ZrSiO_4$). Additives have to help or at least not hinder glass formation while providing some benefit to one of the processing criteria (e.g., electrical

conductivity, viscosity) and/or product performance metrics (e.g., chemical durability). Additives including Zr, Al, Sn, and Si improve the chemical durability but increase viscosity. Alkali and alkaline-earth additions reduce viscosity but do not help chemical durability. It is desired to be able to have a component which improves durability without increasing viscosity, and so hematite (Fe_2O_3) is added to Hanford LAW glass for this purpose [Vienna, 2021]. The boron source, here borax ($Na_2B_4O_7{\cdot}10H_2O$) generally also fulfills this role but can harm chemical durability when added in large concentrations. Additives are summarized in Table 3.

3.5. *Alternative glass systems*

The waste loading in a particular glass system can be limited in order to obtain a homogeneous glass at the microscopic scale or increased to form GCs with a larger amount of waste. The chemical solubility of major constituents (e.g., MoO_3, ZrO_2, noble metals and lanthanides) of the spent nuclear fuel (SNF)-derived waste stream in silicate melts is generally low (1.0–2.5 wt%), and this severely limits the waste loading to an undesirably low level of ~18 wt% in borosilicate glasses. While the majority of the aforementioned discussion is focused on borosilicate glasses, which are the overwhelmingly preferred glass matrices for nuclear waste vitrification [National Research Council, Committee on Waste Forms Technology and Performance, 2011], there are other glass systems which have been considered or used for waste vitrification.

Phosphate glass, in particular, has been particularly important in the former Soviet Union, for immobilizing HLW from Mayak [Laverov et al., 2013, Ojovan and Lee, 2011, Tracy et al., 2021]. Alternative host matrices, such as the iron phosphate glasses [Stefanovsky et al., 2017a] and lead iron phosphate glasses [Sales and Boatner, 1984], can offer a way of overcoming these shortcomings, since phosphate glasses have a much higher solubility for constituents such as halides, molybdenum, and zirconium. Research has suggested that iron phosphate waste forms can increase radioactivity concentrations (>2× greater) that can be safely stored and thereby decrease the total nuclear waste volume (>2× smaller) for storage and disposal [Brow et al., 2020]. However, phosphate glasses are known to react unfavorably with refractory materials [Tracy et al., 2021] including electrodes used in Joule-heated melters [National Research Council, Committee on Waste Forms Technology and Performance, 2011]. Additionally, thermal stability is considered inferior for phosphate glasses compared to borosilicates, so undesired crystallization on cooling may be a problem [Donald, 2016]. Early compositions of phosphate nuclear waste glass had poor chemical durability, but more recent formulations are significantly improved [Stefanovsky et al., 2019]. Some typical compositions of these phosphate glasses are shown elsewhere [Donald, 2016].

4. Glass-ceramic waste forms

A summary of some of the studied crystalline phases, the glass chemistries from which they are precipitated, and their immobilized elements is shown in Table 4. For non-nuclear applications, such as immobilization of hazardous waste or even municipal waste, GCs have also been proposed [Caurant, 2017, Donald, 2010, 2016], though the target crystalline phases are often different. The partitioning of the target elements into crystalline phases is not always complete, but the desire is to incorporate these target elements into chemically durable and radiation-stable phases.

4.1. *Process of fabrication*

For nuclear material immobilization, it is desirable to minimize the number of processing steps, so GCs are typically produced from a melt, where nucleation and growth of crystals happen either at an intermediate hold step or concurrently during cooling (Figure 6) and not as a quench and reheat as done with commercial GCs. The latter, where glasses are quenched then reheated with nucleation and growth steps is referred to as a GC, while the example of a homogeneous glass at melt temperature designed to have controlled crystallization on cooling is not normally referred to as such. In the case of controlled nucleation and growth, the starting point is a single-phase melt or a quenched glass, where the crystals form upon cooling from the melt or heating from the glass. If the crystallization will happen on cooling, it is important to design a system where the nucleation and growth temperature dependencies overlap considerably, which is

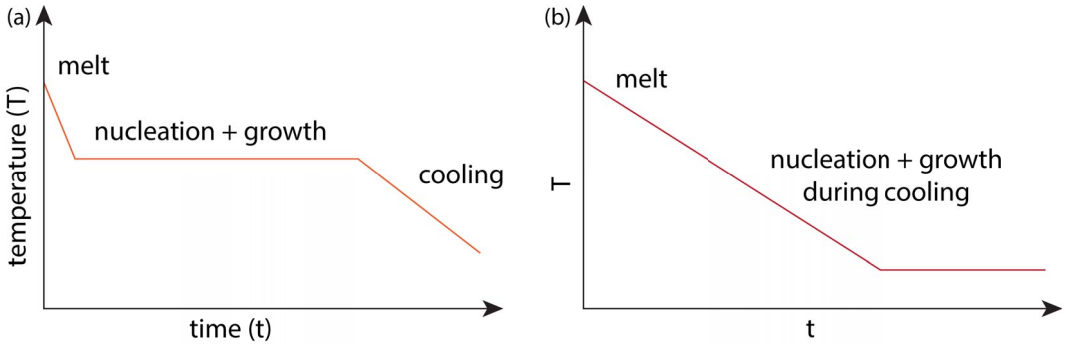

Figure 6. Schemes used for GCs produced from nuclear waste in order to avoid having to reheat quenched glass.

normally not desirable for commercial GCs. Most of the commonly considered nuclear GC systems fall into this latter category, such as those based on zirconolite ($CaZrTi_2O_7$) and pyrochlore ($A_2B_2O_7$). Targeted incorporation is particularly desirable for U, Pu and minor actinides (Am, Np, and Cm), where α emissions may deposit large amounts of energy and create defects or even amorphization of the crystalline phases [Weber et al., 1998].

In another embodiment of this technology, the crystals form at high temperature such as during a hot isostatic press (HIP) or high temperature sintering, and here starting materials are solid calcines generally, sometimes including a fraction of glass binder or at least glass-forming oxides [Vance et al., 2010]. The final product consists of crystalline phases plus a glass phase, and has been demonstrated for U- and Pu-containing pyrochlore GC [Zhang et al., 2013], an apatite GC from high fluorine or chlorine wastes [Raman, 1998, Vance et al., 2012], and a zirconolite GC targeted for Pu residues [Maddrell et al., 2015].

4.2. *Design issues*

Designing a GC to immobilize waste, then, consists of several steps. First, the waste itself must be considered, including its form (solid, liquid), and its overall composition. Problematic components must be identified, both from the standpoint of elements to be immobilized (e.g., Cr^{6+}, Pu) and for the additional elements in the waste that must be properly handled to avoid producing a poorly durable product (e.g., Na). Next, the formula of additives must be determined. This could be dependent on the phases desired for crystallization (e.g., adding TiO_2 to make Synroc-type phases, adding charge compensators to facilitate partitioning of a given element into a target crystalline phase) or adding glass formers to enable production of a high quality glassy matrix (e.g., SiO_2, B_2O_3). Next, the thermal profile must be considered, accounting for the physical form of the waste, the desired method of mixing with additives, and the thermal treatment process (e.g., melt crystallization or HIP). Each of these steps will be described more fully in the following.

A further consideration involves the flexibility of a waste form to accommodate *fluctuations in waste composition* [Marples, 1988]. For instance, it may be desirable to create a GC waste form from non-separated waste, as was the case with attempts for celsian and fresnoite systems [Donald, 2010]. On the other hand, better performance for specific wastes may be achieved by using separated waste streams, such as the α-emitting Pu and minor actinides (An), which may benefit from a GC with a single zirconolite or apatite phase [Caurant et al., 2009]. Since α particles and the corresponding lower energy recoil nucleus deposit all their energy in a very short distance in the material, this can result in volume expansion due to swelling and helium bubble creation and amorphization of some crystalline phases [Weber et al., 1998]. Reliance on studies of natural analogue crystals containing Th or U has helped to underpin predictions of long-term stability of An-containing crystals [Ewing, 1999, Lumpkin, 2006, Weber et al., 1997]. Additionally, beta and gamma decay of important high yield, medium-lived fission products like ^{137}Cs (to ^{137}Ba) and ^{90}Sr (to ^{90}Y then ^{90}Zr) requires consideration of the effects of high decay heat,

chemical change, and possible amorphization on any crystal structure incorporating these elements [Jiang et al., 2014, Marples, 1988, Tang et al., 2014].

Some of the more desirable crystalline phases, particularly for An, are *flexible structures* that can accommodate a large variety of ions in multiple crystallographic sites, and examples include pyrochlore, zirconolite, and apatite. This flexibility allows a certain intrinsic tolerance to variations in the waste stream chemistry. The solubility of target ions in the crystalline phase must be considered, along with the partitioning of elements between the crystalline and residual glass phases [Zhang et al., 2013].

In designing a nuclear GC, one must account for the *desired crystalline phases* and a *suitable melt chemistry* for the processing method selected. Most of the GC systems considered are based on silicate or borosilicate chemistries [Donald, 2010, Donald et al., 1997], but a few phosphate glass systems have been explored [Bart et al., 1998, Raman, 2000]. Subtle changes in the rest of the glass chemistry may also cause critical differences in the phases precipitated. For example, in the Mo-containing GC system it has been shown that the additions of B_2O_3 affect the availability of Na_2O to form undesirable water-soluble alkali molybdate phases, resulting in the preferential production of durable alkaline-earth molybdate phases like powellite ($CaMoO_4$) [Caurant et al., 2010].

Often particular oxides, such as TiO_2, ZrO_2, and Al_2O_3, must be added in large fractions to ensure the desired durable crystalline phases are formed, such as for the titanate, zirconate, and aluminosilicate phases. TiO_2 and ZrO_2 are often added to commercial GCs as nucleating agents [Höche et al., 2012]. In nuclear waste GC, high liquidus temperature oxides (such as the TiO_2, ZrO_2, and noble metal oxides RuO_2 and PdO) may also act as nucleation sites for crystals, although, in many cases, these elements are incorporated into the desired crystalline phases.

Finally, the GC waste form must be economically producible and have reasonable physical properties for processing and storage. From a processing standpoint, the electrical conductivity needs to be high enough to maintain good melting if a Joule-heated ceramic melter or cold crucible induction melter are to be used. In one recent example, scale-up to melter tests required a formulation change where Li_2O was added to increase electrical conductivity of the glass melt to accommodate melter limitations [Crum et al., 2014]. Other schemes of GC fabrication, such as high temperature HIP, may not necessitate this requirement.

At the end of the processing, the waste form must maintain good thermal stability and mechanical properties. Thermal stresses accumulated during cooling, as well as thermal expansion mismatch between crystalline phases and residual glasses, can cause undesirable cracking or preferential dissolution at interfaces. At some point, optimization is necessary, once initial experimental trials have established some of the partitioning, and chemical durability measurements have been performed on the GC as well as its individual components. For instance, there may be some relationship between the temperature of crystallization of a phase, its anisotropic thermal expansion coefficients, and the glass transition temperature. These connections may result in stresses at the crystal–glass boundaries which can cause selective leaching [Crum et al., 2016], and these factors need to be considered in addition to the individual durabilities of the crystalline and residual glass phases [McClane et al., 2021, Neeway et al., 2018]. These interaction factors depend on the actual crystallization sequence, the distribution and size of the crystalline phases, and by extension, the cooling rates [Asmussen et al., 2017].

4.3. *Mechanisms of phase separation and crystallization of GCs*

The development of controlled spontaneously crystallizing GC materials is an attractive way to increase the waste loading. This approach has been already demonstrated for the vitrification of U–Mo waste solution enriched in MoO_3 [Pinet et al., 2019] and as an alternative for immobilizing non-fissionable products obtained from aqueous reprocessing [Crum et al., 2014, 2012, McCloy and Goel, 2017]. Design of the waste form and its evolution during processing, however, demands greater attention to ensure the required quality (durability, thermal stability). The mechanisms of phase separation and crystallization have to be carefully understood and controlled at each step in the processing. Figure 7 shows an illustration of the main mechanisms of phase separation and crystallization as obtained by nucleation and growth.

The schematic in Figure 7 describes the evolution of the morphologies obtained after different processes and by the different steps of equilibrium in the free energy-composition diagram at a temperature above the phase separation (immiscibility) temperature. For a liquid of composition **L0**, represented in a XY binary composition diagram, the first step is given by the equilibrium between the liquids **A** and **B** along tangent **AB** of the change in Gibbs free energy (ΔG).

Liquid–liquid phase separation leads to two different phases: one highly enriched in X (phase **A**), containing a small amount of Y, and the other enriched in Y (phase **B**), containing a residual amount of X. This process is characterized by the step **a** microstructure, corresponding to the formation of spherical separated phases **B** embedded in a residual phase **A**.

Depending on the relative stability of **A** and **B**, below the liquidus temperature, **B** can totally crystallize to form **B′** (step **c1**) or to remain liquid. Either solid or liquid can act as a nucleation agent to lead to the complete crystallization of the major liquid **A** in a more stable phase **A′** (steps **c2** and **d1**).

Liquid separated phase **B** can also grow in size (step **b1**) and lead to the formation of secondary liquid separated phases. In this case, a new equilibrium is established along tangent **CD**. In accordance with the mass balance (**B** → **C** + **D**), phase **B** evolves (step **b2**) to a new equilibrium with the crystallization of phase **C** and the formation of a new vitreous phase **D** (step **b3**) in the form of beads. This results in the formation of a complex phase assemblage of crystalline phases and glassy phases in the initial liquid separated phase **B**. In this case, **A** never crystallizes, and remains vitreous after cooling. This morphology has been shown in the U–Mo glass [Schuller et al., 2008] and in simple borosilicate glass compositions containing MoO_3 [Brehault et al., 2018, Kroeker et al., 2016]. In this process, separated phase **B** can also act as a nucleation agent (same process as steps **c2** and **d1**) and can lead to the crystallization of the residual matrix **A**.

The initial liquid **L0** can also be destabilized by an initial crystallization and lead to another liquid **L1**. In this case, the precipitated crystal acts as a nucleating agent to promote liquid–liquid phase separation. A clear example is the impact of interaction between trivalent lanthanide (Ln^{3+}) ions and molybdate ions on the crystallization behavior of an alkali/alkaline-earth alumino-borosilicate glass [Chouard et al., 2016] (Figure 8). When Nd^{3+} is below its solubility limit in this glass system, the Ln^{3+} ions keep the Mo-rich glass from phase separating. However, when there is excess Nd^{3+}, an oxyapatite phase is precipitated, which locally depletes the residual glass of Nd^{3+}, causing phase separation of the Mo-rich liquid and subsequent nucleation of more oxyapatite crystals. This last example points to the complexity of phase separation and crystallization mechanisms (controlled by glass chemistry), and emphasizes their synergetic effects on the microstructure of crystallized glasses.

4.4. *Glass-ceramic families*

As may be apparent from the discussion thus far, many GC and glass-crystalline materials systems have been considered for nuclear waste immobilization. The large diversity of crystalline phases that have been considered is indicative of the compositional complexity and variability of wastes. A summary of some of the crystalline phases is shown in Table 4, for immobilization of alkaline earths (Ba, Sr), alkali (Cs), halides (Hd: Cl, I), molybdenum, and actinides (An)/lanthanides (Ln). For early experiments on phases which will ultimately contain An, lanthanides (Ln^{3+}) are often used as surrogates; in particular, Nd^{3+} is frequently used as a surrogate for trivalent minor An, and Ce^{4+} as a surrogate for tetravalent U or Pu [Caurant et al., 2009]. However, it should be noted that though Ce^{4+} is a good An analogue due to its charge and ionic radius, it readily oxidizes to Ce^{3+} in many cases, and other ions such as Hf^{4+} may be better surrogates.

Probably the most research on ceramic phases for radioactive waste immobilization has focused on the transuranic actinides (e.g., Pu, Np, Cm), as isotopes of these have long half-lives and deposit large amounts of energy as they decay by alpha or beta processes [Weber et al., 1998]. Additionally, today there exists a large amount of aging separated Pu in the UK and other countries which have become national priority for immobilization for environmental and security reasons [Ebbinghaus, 1999, Hyatt, 2017]. Additionally, the crystalline phases that accommodate large actinide (An) ions tend also to be suitable for lanthanides (Ln), which are abundant fission products in reprocessed used nuclear fuel. For these reasons, much research has focused on

Table 4. Summary of important phases in nuclear waste glass-ceramics

Crystalline phase	Nominal stoichiometry	Glass systems	References
Actinide/lanthanide phases			
Oxides			
Baddeleyite	ZrO_2 [An, Ln in Zr site; can be monoclinic, tetragonal, or cubic]	Na_2O–CaO–Al_2O_3–B_2O_3–MoO_3–Ln_2O_3–ZrO_2	Chen et al. [2020], Patil et al. [2018]
Cerianite	CeO_2	Na_2O–CaO–Al_2O_3–B_2O_3–MoO_3–CeO_2–ZrO_2	Crum et al. [2012], Patil et al. [2018]
Rutile	TiO_2	Synroc phase	Ringwood et al. [1979b]
Silicates			
Zircon	$ZrSiO_4$	Minor phase	Chen et al. [2020], Schuller et al. [2011]
Apatite (silicate), Britholite	$Ca_2Ln_8(SiO_4)_6O_2$	Na_2O–Al_2O_3–B_2O_3–Ln_2O_3 SiO_2–Al_2O_3–B_2O_3–CaO–Na_2O–ZrO_2–Nd_2O_3	Zhao et al. [2001] Caurant et al. [2006]
Keiviite	$Ln_2Si_2O_7$	CaO–Na_2O–SiO_2–B_2O_3–Al_2O_3–ZrO_2–MoO_3–Ln_2O_3	Chen et al. [2020], Patil et al. [2018]
Ln borosilicate	$Ln_3BSi_2O_{10}$	CaO–Na_2O–SiO_2–B_2O_3–Al_2O_3–ZrO_2–MoO_3–Ln_2O_3	Chen et al. [2020], Patil et al. [2018]
Titanates			
Pyrochlore	$Ln_2Ti_2O_7$ or $(Ca,Ln,U)_2(Ti,Hf)_2O_7$ or $(Na,Ca)_2Nb_2O_6F$	SiO_2–Al_2O_3–B_2O_3–Na_2O–[CaO–TiO_2–Y_2O_3–Gd_2O_3] SiO_2–Al_2O_3–B_2O_3–Na_2O–[CaO–UO_2–TiO_2] SiO_2–Al_2O_3–B_2O_3–Na_2O–CaF_2–[CaO–UO_2–TiO_2] SiO_2–Al_2O_3–B_2O_3–Na_2O–CaF_2–[CaO–UO_2–PuO_2–TiO_2–HfO_2–Gd_2O_3] SiO_2–Al_2O_3–B_2O_3–Na_2O–[CaF_2–Nb_2O_5–TiO_2–Nd_2O_3]	Zhang et al. [2017b] Carter et al. [2009] Feng et al. [2019] Zhang et al. [2013] Wu et al. [2020]
Brannerite	$(U,Ln,Ca)Ti_2O_6$	SiO_2–Al_2O_3–B_2O_3–Na_2O–[UO_2–TiO_2–CaO–Ln_2O_3–CeO_2] SiO_2–Al_2O_3–B_2O_3–Na_2O–[UiO_2–TiO_2]	Zhang et al. [2018, 2017b, 2019] Dixon Wilkins et al. [2020]
Murataite	$Zn(Ca,Mn)_2(Fe,Al)_4Ti_3O_{16}$	No reported GC systems	Stefanovsky and Yudintsev [2016]
Loveringite	$(Ca,Ce,U)(Ti,Fe,Cr,Mg)_{21}O_{38}$	No reported GC systems	Lumpkin and Geisler-Wierwille [2012]
Perovskite	$CaTiO_3$	Minor phase, often in zirconolite GC systems	Loiseau and Caurant [2010], Lumpkin [2006], Wu et al. [2018]
Sphene (Titanite)	$CaTiSiO_5$	Al_2O_3–ZrO_2–Nd_2O_3–[CaO–SiO_2–TiO_2] Na_2O–Al_2O_3–[CaO–SiO_2–TiO_2] [CaO–SiO_2–TiO_2]	Caurant et al. [2006] Hayward [1988a] Jelena et al. [2020]
Crichtonite	$Ca(U,Ti,Fe,Cr,Mg)_{21}O_{38}$	Minor phase with murataite; no reported GC systems	Yudintsev et al. [2019]

(continued on next page)

Table 4. (continued)

Crystalline phase	Nominal stoichiometry	Glass systems	References
Zirconates			
		SiO_2–Al_2O–Nd_2O_3–[CaO–TiO_2–ZrO_2]	Caurant et al. [2006]
		SiO_2–Al_2O_3–[CaO–TiO_2–ZrO_2]	Loiseau et al. [2003a]
		SiO_2–Al_2O_3–B_2O_3–PbO–K_2O–[CaO–TiO_2–ZrO_2]	Mahmoudysepehr and Marghussian [2009]
		SiO_2–Al_2O_3–B_2O_3–Gd_2O_3–Na_2O–CaF_2–[CaO–TiO_2–ZrO_2]	Maddrell et al. [2015]
Zirconolite	$CaZrTi_2O_7$	SiO_2–B_2O_3–Nd_2O_3–Na_2O–BaO–[CaO–TiO_2–ZrO_2]	Li et al. [2015], Wu et al. [2016a, 2018]
		SiO_2–Al_2O_3–Nd_2O_3–Na_2O–[CaO–TiO_2–ZrO_2]	Liao et al. [2017]
		SiO_2–Al_2O_3–Na_2O–[CaO–TiO_2–ZrO_2]	Maddrell et al. [2017]
		SiO_2–Al_2O_3–B_2O_3–Na_2O–[CaO–TiO_2–ZrO_2]	Maddrell et al. [2015], Thornber et al. [2017]
		SiO_2–Al_2O_3–B_2O_3–Na_2O–CeO_2–[CaO–TiO_2–ZrO_2]	Zhu et al. [2020]
Garnet	$(Al,Si,Fe,Ln)_3(Ca,Zr)_5O_{12}$	No reported GC systems	Stefanovsky and Yudintsev [2016]
Phosphates			
Monazite	$LnPO_4$	La metaphosphate: La_2O_3–P_2O_5–Nd_2O_3–ZrO_2–CeO_2–MoO_3–Fe_2O_3	He et al. [2008]
		Fe phosphate: P_2O_5–Fe_2O_3–(B_2O_3–TiO_2)–(CeO_2–Gd_2O_3–La_2O_3–Nd_2O_3)	Asuvathraman et al. [2015], Deng et al. [2018], Wang et al. [2016, 2020b,c]
Apatite (phosphate)	$(Ca,Ln)_{10}(PO_4)_6O_2$	MgO–CaO–P_2O_5–SiO_2–Nd_2O_3	Bart et al. [1998]
Kosnarite	$(K,Na)Zr_2(PO_4)_3$	P_2O_5–Fe_2O_3–Na_2O–ZrO_2	Liu et al. [2019], Wang et al. [2020a]
Vitusite	$Na_3Ce(PO_4)_2$	SiO_2–B_2O_3–P_2O_5–Na_2O–Nd_2O_3–CeO_2	Kim and Heo [2015], Kim et al. [2017]
Whitlockite	$Ca_8MgNd(PO_4)_7$	Minor phase	Bart et al. [1998]

(continued on next page)

Table 4. (continued)

Crystalline phase	Nominal stoichiometry	Glass systems	References
Barium/strontium/cesium phases			
Celsian	$BaAl_2Si_2O_8$	B_2O_3–CaO–Na_2O–Li_2O–TiO_2–ZnO–[BaO–Al_2O_3–SiO_2]	Hayward [1988a]
Fresnoite	$BaTiSi_2O_8$	CaO–MgO–Al_2O_3–ZnO–[BaO–TiO_2–SiO_2]	Hayward [1988a]
Scheelite	$(Ba,Sr)MoO_4$	Minor phase	Hayward [1988a]
Perovskite	$(Ca,Sr)TiO_3$	Minor phase	Hayward [1988a]
Ba-priderite	$BaFe_2Ti_6O_{16}$	Minor phase	Hayward [1988a]
Hollandite	$BaAl_2Ti_6O_{16}$	Synroc phase	Ringwood et al. [1979b]
Pollucite	$CsAlSi_2O_6$	B_2O_3–Na_2O–CaO–BaO–P_2O_5–ZrO_2–[Cs_2O–Al_2O_3–SiO_2]	Hayward [1988a], Kissinger et al. [2021], Strachan and Schultz [1976]
		B_2O_3–Na_2O–CaO–[Cs_2O–Al_2O_3–SiO_2]	Yang et al. [2021]
		B_2O_3–Na_2O–[Cs_2O–Al_2O_3–SiO_2]	He et al. [2020]
Cs-pyrochlore	$CsTiNb_6O_{18}$	HIP of crystalline silicotitanate ion exchange media	Chen et al. [2018]
Cs-leucite	$(Cs,K)Al_2O_6$	HIP of chabazite ion exchange media	Gardner et al. [2021]
Molybdenum phases			
Powellite	$(Ca,Sr)MoO_4$	Minor phase	Crum et al. [2014]
Scheelite	$(Ba,Sr)MoO_4$	Minor phase	Brinkman et al. [2013], Crum et al. [2014], Hayward [1988a]
Mo-nosean	$Na_8Al_6MoO_4(SiO_4)_6$	Minor phase	Hayward [1988b]
Halide phases			
Apatite	$(Ca,Pb)_5(PO_4,VO_4)_3(F,Cl,I)$	SiO_2–P_2O_5–Al_2O_3–B_2O_3–ZrO_2–CaF_2–Na_2O–CaO–MgO	Raman [1998]
		Fe_2O_3–P_2O_5–SrF_2 [HIP: fluorapatite]	Gregg et al. [2020b], Zhou et al. [2021]

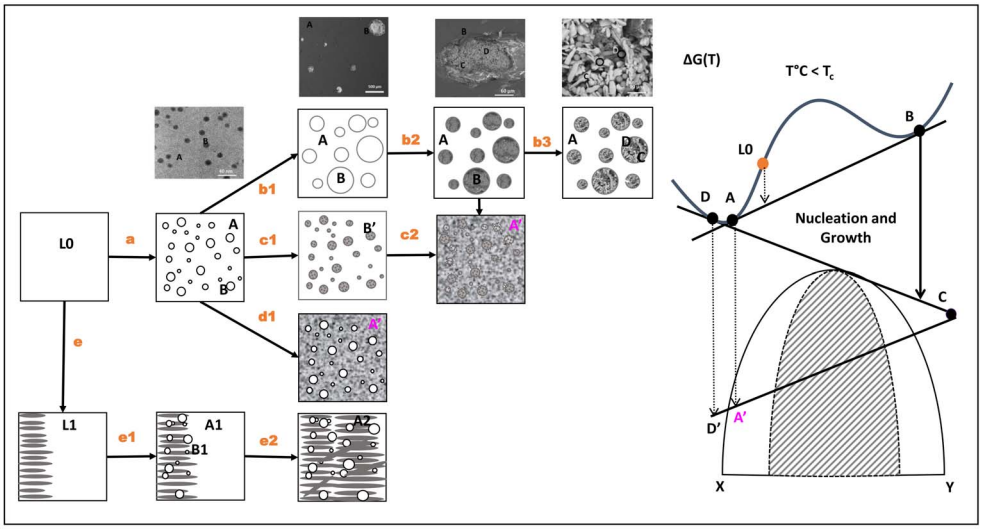

Figure 7. Possible phase separation and crystallization mechanisms obtained by nucleation and growth processes in nuclear and industrial wastes, based on original work of Gutzow [1980a,b] and more recent work of Chouard et al. [2016] and Schuller [2017].

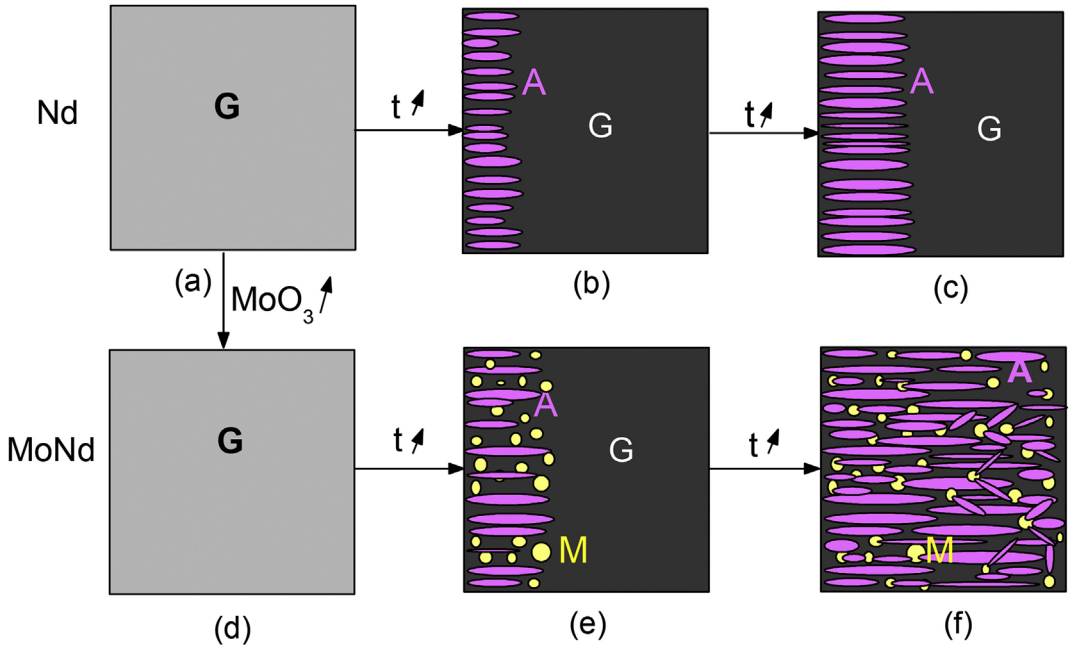

Figure 8. Example of the effect of phase separation on crystallization in rare earth (Nd) and molybdenum (Mo) containing nuclear waste glasses; in systems containing only Nd, the glass (G) forms surface crystallization of oxyapatite (A); in compositions with Mo and Nd, the crystallization of apatite promotes phase separation of molybdate (M) droplets, which further nucleates more apatite crystals. From Chouard et al. [2016], copyright Elsevier, used with permission.

understanding the crystalline structure and An/Ln accommodation of a number of mineral phases, and in many cases GC routes to waste form fabrication have been proposed.

Rather than detail all these studies, we summarize them in Table 4, and briefly below. We categorize the systems as primarily phosphate, silicate, zirconate/titanate, or Cs/Ba/Sr phases. For industrial wastes, we describe them together first, in terms of the typical phases formed, without doing a comprehensive study of the literature here.

4.4.1. *Silicates and related phases: industrial waste glass-ceramics*

Nearly all of the relevant wastes which have been considered for vitrification fall within the overall SiO_2–Al_2O_3–CaO system [Caurant, 2017, Karamanov, 2009]. For this reason, normally few additives are needed to make glass-forming systems, when the waste is of this type. The main difference in composition between incinerator ash (IA), coal fly ash (CFA), sewage sludge (SS), and slag from the iron industry (IS) is the relative amounts of these three oxides. IA and IS have relatively higher CaO and lower SiO_2, with IA having some Al_2O_3 and Fe_2O_3. CFA and SS have similar compositions, with high SiO_2 and low CaO with relatively high Al_2O_3. The only exception to this is Zn hydrometallurgical waste (either jarosite or goethite based) which is mostly Fe_2O_3, so requiring a significant amount of additional SiO_2 to form glass. Chlorides and sulfates are present in some wastes, like fly ash, which can give rise to similar problems with molten salts [Caurant, 2017], as described in the yellow phase/sulfate section.

The emphasis in industrial waste GC has been to achieve good thermal and mechanical properties (toughness, abrasion resistance) along with favorable aesthetics (color, texture) [Karamanov, 2009]. Rarely are studies performed to assess the immobilization of hazardous elements (such as heavy metals) through chemical durability tests, which show a stark contrast with typical studies for nuclear waste GC [Caurant, 2017]. All the typical methods for producing GC have been explored with industrial wastes, including quenching followed by nucleation and growth, crystallizing from a melt on cooling, and sintering of glass powders [Caurant, 2017, Karamanov, 2009]. Several commercial products were produced at one point from metallurgical wastes, including Slagsital [Holland and Beall, 2012] and Slagceram [Karamanov, 2009]. Nucleation of crystals can happen from phase separation, such as with high P_2O_5, from oxides like Fe_2O_3 or Cr_2O_3 in the waste, from added nucleating agents like TiO_2, or on glass particle surfaces [Caurant, 2017, Holland and Beall, 2012, Karamanov, 2009].

The crystalline phases that form in such GCs are therefore silicates [Isa, 2011]: typically calcium silicates (wollastonite, $CaSiO_3$), pyroxenes (diopside, $MgCaSi_2O_6$; hedenbergite, $CaFeSi_2O_6$; augite, see below), aluminosilicates (gehlenite/akermanite, $Ca_2Al_2SiO_7$–$Ca_2MgSi_2O_7$; cordierite, $(Mg,Fe)_2Al(Si_5AlO_{18})$; anorthite $CaAl_2Si_2O_8$,), and sometimes spinel (including magnetite, Fe_3O_4; franklinite, $ZnFe_2O_4$; and other mixed ferrites). For example, **augite**, $(Ca,Mg,Fe^{2+})Si_2O_6$, is a major crystalline phase produced in GCs for immobilizing lanthanide-containing mining wastes, where they crystallize from CaO–MgO–SiO_2–Al_2O_3 glasses containing the mixed lanthanide oxide waste, and La substitutes for Ca in the clinopyroxene augite phase [Chen et al., 2019a]. Related diopside-based GCs have also been proposed for immobilization of heavy metals Pb and Cd from incinerator waste [Krausova et al., 2016].

4.4.2. *Silicates and related phases: nuclear waste glass-ceramics*

Similar composition, basalt-based GCs have been investigated from the beginning for nuclear waste immobilization [Hayward, 1988a, Martinez et al., 1987], focusing on remelting natural basaltic rock along with calcined waste oxides, to produce pyroxenes like augite along with hematite (Fe_2O_3) or magnetite and sometimes other spinels ($NiFe_2O_4$) and powellite. Here augite or another pyroxene was a major phase designed to incorporate transuranics [Hayward, 1988a].

Much recent work has been performed looking at the crystallization of silicate phases from alumino-boro-silicate glasses. French scientists investigated these systems for immobilization of U–Mo glass compositions and US scientists for a proposed GC produced from aqueous reprocessed commercial UO_2 fuel [McCloy et al., 2019a]. In both cases, the GC were to be produced in a cold crucible induction melter, where nucleation and growth happened on cooling [Caurant et al., 2009, Crum et al., 2014, Schuller et al., 2011]. The primary phases of interest in this system are silicate oxyapatite, nominally $Ca_2Ln_8(SiO_4)_6O_2$, for immobilizing lanthanide fission products and actinides, and powellite $CaMoO_4$ for immobilizing Mo and Sr/Ba

[Crum et al., 2012]. Numerous studies have been made on single-phase ceramics and GCs of oxyapatite and powellite studying their chemical durability and radiation damage behavior [Asmussen et al., 2017, Brinkman et al., 2013, Chouard et al., 2019, Crum et al., 2016, Fahey et al., 1985, Neeway et al., 2018, Peterson et al., 2018, Tang et al., 2014, Weber et al., 1997].

The **powellite** (nominally $CaMoO_4$) structure has been shown to be flexible to accommodate multiple waste ions when crystallized out from a complex nuclear waste glass. Chief among these is the incorporation of Ba and Sr, which have been shown to separate into two different powellite phases, one with (Ba,Sr) and the other with (Ca,Sr) [Crum et al., 2014]. Powellite can also incorporate a significant amount of lanthanide elements along with Na_2O for charge compensation [Patil et al., 2018]. This proximal location of lanthanide and molybdenum ions in the crystal supports recent assertions about the role of rare earths in aiding the dispersion of molybdate ions in these glasses [Kamat, 2021]. The nucleation of powellite happens at high temperature through a phase separation process in a Mo-rich liquid [McCloy et al., 2019b], as discussed previously.

Oxyapatite can likewise incorporate many metal ions. Trivalent americium has specifically been demonstrated to partition to an oxyapatite phase from alumino-boro-silicate GC [Bardez-Giboire et al., 2017]. These oxyapatites have been shown by electron microprobe to accommodate significant amounts of ZrO_2, B_2O_3, and Na_2O from the glass [McCloy et al., 2019b, Patil et al., 2018]. There are related natural apatite family minerals which are primarily silicate (britholite) or which contain both silicate and borate in the structure (tritomite, caryocerite) [Chen et al., 2020]. Other crystalline phases can nucleate oxyapatite from these glasses, including powellite as discussed above [Chouard et al., 2016], as well as ruthenium dioxide [Kamat et al., 2020].

Other silicate or borosilicate phases can form either with oxyapatite or instead of it, depending on the glass composition. It was shown, for instance, that small trivalent lanthanide ions (Ho, Y, Tm, Yb, Lu) result in the preferential formation of **keiviite** ($Ln_2Si_2O_7$) [Chen et al., 2019a, Patil et al., 2018]. This phase due to its crystal chemistry can incorporate large amounts of ZrO_2 as well as some CaO and B_2O_3 [Chen et al., 2020]. In rare cases with peralkaline borosilicates [Chong et al., 2021, Crum et al., 2014, Kissinger et al., 2021] and frequently with peraluminous compositions [Chen et al., 2020], a **lanthanide borosilicate** phase $Ln_3BSi_2O_{10}$ will form. This phase incorporates some B_2O_3 and ZrO_2, and forms with the larger lanthanides (La to Gd) in CaO–Na_2O–SiO_2–B_2O_3–Al_2O_3–ZrO_2–MoO_3–Ln_2O_3 peraluminous glasses rather than oxyapatite [Chen et al., 2020]. In this same glass series, smaller lanthanides (Tb to Lu) instead form keiviite or oxyapatite plus a lanthanide borate phase [Chen et al., 2020]. The borate phase is nominally $LnBO_3$, but can incorporate CaO, ZrO_2, and some SiO_2.

Finally, nuclear GC often also contain a specific Zr phase, normally a form of $ZrSiO_4$ (**zircon**) or ZrO_2 (**zirconia**) [Chen et al., 2020]. The ZrO_2 phase can incorporate a large amount of lanthanide, changing from the monoclinic baddeleyite to a tetragonal or cubic fluorite structure [Chen et al., 2020]. Cubic zirconia occurs naturally in the mineral tazheranite, written as $(Zr,Ti,Ca)O_{2-x}$ or $CaTiZr_2O_8$ [Stefanovsky and Yudintsev, 2016]. Both zircon and zirconia have been studied as single-phase ceramics for plutonium immobilization [Ewing et al., 1995, Gong et al., 2000]. The nuclear waste community has extensively studied zircon for the following reasons [Ewing, 1994, Ewing et al., 1987, Ewing and Haaker, 1980, Weber, 1990]. Zircon has a propensity for incorporation of uranium, thorium, and lanthanides in natural minerals, and it amorphizes over time due to radiation damage (metamictization). Additionally, natural zircon crystals can be precisely dated due to uranium decay, thus giving the ability to obtain rates for radiation damage. Finally, the structure of zircon is related to other important crystal phases like the phosphate-mineral monazite.

4.4.3. *Zirconates and titanates*

The selection of a crystalline phase to immobilize radionuclides which undergo alpha decay or fission at least partially relies on their radiation damage tolerance. One consequence of radiation damage is the production of amorphized structures in previously crystalline materials [Weber et al., 1998]. This metamictization has been studied for natural materials of various chemistries, including silicates, phosphates, titanates, and zirconates. Theoretical studies have shown that the resistance to amorphization can be understood as being related to the relative

covalent character of relevant bonds, at least for oxides [Trachenko, 2004, Trachenko et al., 2005]. This explains the relative propensity of phosphates and silicates to amorphize at lower doses than titanates, for example. Zirconates, being the most ionic, exhibit the least tendency to amorphize, and this corresponds also to their poor glass-forming ability compared to the other systems [Trachenko, 2004]. Thus particularly for single-phase ceramics, but also some GCs where large amounts of energy deposition are expected, such as in separated Pu streams, zirconate phases may be preferable if amorphization is undesirable.

In the previous section, it was discussed that Zr-containing phases are often present in aluminoboro-silicate GC designed to immobilize reprocessing waste. Additionally, there is an important set of GC studied specifically for the immobilization of plutonium and minor actinides within the phase of **zirconolite**, nominally $CaZrTi_2O_7$, but incorporating in nature significant metal substitutions [Blackburn et al., 2021, Omel'yanenko et al., 2007]. Related mineral species are generally considered as "zirconolites" including monoclinic, trigonal, and orthorhombic phases including related minerals like zirkelite [cubic $(Ca,Th,Ce)Zr(Ti,Nb)_2O_7$ or $(Ti,Ca,Zr)O_{2-x}$] [Stefanovsky and Yudintsev, 2016]. Zirconolite and the related cubic pyrochlore (see below) have been among the most studied crystalline phases for nuclear waste ceramics, as zirconolite is one of the key phases produced in the multiphase titanate-based ceramic waste form called Synroc [Gregg et al., 2020a, Ringwood et al., 1979b, Vance, 1994, Vance et al., 2017].

Zirconolite-based GCs have been studied for at least two decades, with detailed crystallization studies of $CaO–Al_2O_3–SiO_2$ with TiO_2 and ZrO_2 having been performed early on [Loiseau et al., 2003a,b]. Lanthanide oxides are also added, and these incorporate into the zirconolite structure [Caurant et al., 2006]. Much of this work, including control of surface versus bulk crystallization, was summarized in a book in 2009 [Caurant et al., 2009]. In zirconolites for immobilizing Pu, Hf is often added to control criticality, and it substitutes on the Zr site [Caurant et al., 2007b]. In systems forming zirconolite where multiple lanthanides and/or actinides are present, zirconolite tends to prefer smaller Ln ions (e.g., trivalent Y, Gd, Eu) and An^{4+} while the **perovskite** phase (nominally $CaTiO_3$) tends to preferentially accommodate large Ln ions (e.g., trivalent Nd, Ce, La) and An^{3+} species [Lumpkin, 2006]. This partitioning is important, since though perovskite has a higher amorphization threshold than zirconolite, its chemical durability is considerably lower [Blackburn and Hyatt, 2021, Lumpkin, 2006].

While early work was focused on quenching glass followed by nucleation and growth of zirconolite, recent efforts have focused on HIP. HIP was proposed for halide-contaminated Pu wastes from Sellafield, UK [Stewart et al., 2013]. In $Na_2O–Al_2O_3–B_2O_3–SiO_2–CaO–TiO_2–ZrO_2–CaF_2–Gd_2O_3$ systems, it was found that as Al/B ratio in the composition decreased, zirconolite no longer formed, but rather sphene ($CaTiSiO_5$), zircon, and rutile (TiO_2) [Maddrell et al., 2015]. Many other recent studies have been made on zirconolite GC systems [Li et al., 2015, Wu et al., 2016b], including those focusing on phase evolution over time [Maddrell et al., 2017], effect of glass composition [Maddrell et al., 2015], and effect of redox conditions [Zhang et al., 2017a]. In some studies, a precursor ceramic zirconolite phase is used, then reacted with glass powder precursors, which is hence not a true GC by the definition espoused here [Kong et al., 2019].

Sphene (also called titanite) GCs were explored in some detail by the Canadian scientific community to immobilize the radioactive waste from the CANDU (Canada Deuterium Uranium) reactors [Hayward, 1988a,b]. GCs were formulated from the $Na_2O–Al_2O_3–SiO_2–CaO–TiO_2$ + waste oxide system, with the sphene ($CaTiSiO_5$) crystal designed to accept a large variety of waste cations, leaving a durable aluminosilicate glass matrix. Some minor phases produced in sphene GC include pyrochlore, fluorite, wollastonite, powellite, anorthite, fresnoite, perovskite, and perrierite [$(Ca,U,Ln)_2Ti_2Si_2O_{11}$] [Hayward, 1988b]. Sphene was an attractive matrix for incorporating waste components due to its known chemical durability even in brines and after irradiation-induced amorphization, as observed in naturally metamict samples [Hayward, 1988a]. Only limited work has been published in recent years on sphene systems, notably GCs produced from isochemical glasses [Jelena et al., 2020]. Sphene can sometimes form on zirconolite GC as an undesirable surface-crystallized phase [Loiseau and Caurant, 2010].

A number of other titanate phases have been investigated for nuclear waste immobilization in the context of multiphase ceramic waste forms known as Synroc, originally developed in Australia [Ringwood et al., 1988, 1979a,b]. The Synroc systems were mostly based on titanate minerals and were designed for HIP [Vance et al., 2017], though melt-derived Synrocs have also been reported [Amoroso et al., 2017, Tumurugoti et al., 2016]. The target phases are usually hollandite (nominally $BaAl_2Ti_6O_{16}$), zirconolite, pyrochlore (nominally $(An,Ln)Ti_2O_7$), and perovskite ($CaTiO_3$). Waste form design generally targets immobilization of Cs and Rb with hollandite, rare earths and actinides with zirconolite and perovskite, Sr with perovskite, and platinoid metals and Tc with an alloy phase [Vance et al., 2014]. Usually some Ti oxide phases like rutile (TiO_2) and reduced TiO_{2-x} phases, Magnéli phases Ti_nO_{2n-1}, are also present due to interactions with HIP cans or addition of Ti powder to reduce the oxidation state of metals cations [Carter et al., 1996, Gregg et al., 2020a]. Other minor titanate phases, which can accommodate large ion fission products, lanthanides, and actinides, are sometimes observed, such as loveringite and related minerals of the crichtonite group such as davidite [Lumpkin and Geisler-Wierwille, 2012]. Metals such as Cr and Fe can partition into crichtonite minerals between loveringite, $(Ca,Ce,U)(Ti,Fe,Cr,Mg)_{21}O_{38}$ and davidite $(Ca,Ce,La)(Y,U)(Ti,Fe^{3+})_{20}O_{38}$ [Buykx et al., 1990, Green and Pearson, 1987].

Other than zirconolite, the phase arguably best studied for actinide immobilization is **pyrochlore**. The mineral pyrochlore itself is $(Na,Ca)_2Nb_2O_6(OH,F)$, but the pyrochlore group refers to a number of titanates, zirconates, halfnates, niobates, and tantalates with cubic structures related to fluorite, written as $A_2B_2O_6X$ (where $X = O^{2-}$, OH^-, F^-, or vacancy) [Omel'yanenko et al., 2007, Stefanovsky and Yudintsev, 2016]. In fact, the structures of fluorite solid solution, defective fluorite, and pyrochlore structures can occur in the same binary system depending on the concentration of the two metals [Stefanovsky and Yudintsev, 2016]. Pyrochlore and zirconolite structures often interchange depending on the relative concentrations of metals species and their oxidation state [Aleshin and Roy, 1962, Xu et al., 2004], for example where Ce^{3+} incorporates into zirconolite-4M and perovskite and Ce^{4+} incorporates into pyrochlore [Zhang et al., 2020]. A related cubic structure considered for nuclear waste immobilization is murataite, which consists of two fluorite unit cells together rather than the two for pyrochlore [Stefanovsky and Yudintsev, 2016], though no reports of GC have yet been made. Titanate pyrochlore $(U,Pu,Hf,Gd)_2Ti_2O_7$, having minor phases of zirconolite, rutile, and brannerite, was determined by a US scientific program in the early 2000s as the recommended phase for Pu immobilization due to its good radiation stability and chemical durability [Caurant et al., 2007a, Lee et al., 2006].

Many studies have been made recently on pyrochlore-based GCs. Early reported studies are properly glass composites, with a lead-containing cathode ray tube glass matrix encapsulating $La_2Zr_2O_7$ or $Gd_2Zr_2O_7$ pyrochlore with sintering or hot pressing temperatures below 700 °C [Boccaccini et al., 2003, 2004, Digeos et al., 2003]. Similar studies were made using borosilicate glass matrices and pre-reacted zirconate powders [Pace et al., 2005]. More recent studies have been performed at the Australian Nuclear Science and Technology Organization (ANSTO). Researchers there have produced true GC by the HIP process, starting with oxides or calcined nitrates containing both the glass (Na_2O–Al_2O_3–B_2O_3–SiO_2) and pyrochlore (CaO–UO_2–TiO_2) precursors, then HIPping at a high temperature with some metal powder (Ti, Fe, or Ni) to control the redox [Carter et al., 2009]. Resulting GC showed pyrochlore, brannerite, sphene, rutile, and UO_2 phases [Carter et al., 2009]. Later studies tested the incorporation of CaF_2 and PuO_2 and neutron poisons Gd_2O_3 and HfO_2, but essentially the process was similar, and internal crystallization was demonstrated [Zhang et al., 2013]. Some amount of secondary phases of CaF_2, $USiO_4$, and $Ca_3Al_6Si_2O_{16}$ was noted. Slightly modified processes were used to make Ln (Tb, Yb, Er, or Gd)-Ti precursors by wet chemistry methods making loose agglomerate not requiring milling; this powder was then added to the glass precursor and a cold-press-and-sinter route produced internally crystallized $Ln_2Ti_2O_7$ pyrochlore phases in a glass matrix [Kong et al., 2017a]. A later study focused on $Y_2Ti_2O_7$ and the effect of process parameters such as ratio of glass to ceramic precursors, calcination temperature, and cooling rate [Kong et al., 2017b]. HIP methods have most recently been revisited, and interactions with the stainless steel canister produced mixed Cr/Ti oxides, $CrTi_2O_5$, and Gd-(Si/Ti) oxides crystals

in addition to the desired Y- and Gd-pyrochlore titanate phases in glass [Wei et al., 2019]. Finally, a different group has recently produced $Ca_2Nb_2O_7$-based pyrochlore GC by melting precursors and crystallizing on controlled cooling [Wu et al., 2020]. Uniform microstructures of $(Ca,Na)(Nb,Ti)_2Nd_{0.67}O_6F$ pyrochlore crystals were produced in an aluminoboro-silicate glassy phase, and the overall waste form showed chemical durability comparable to typical HLW borosilicate glasses [Wu et al., 2020].

Brannerite, nominally UTi_2O_6, is structurally composed of Ti and U octahedra, and can substitute Ca, Th, Ln, and other elements by oxidizing some U^{4+} [Lumpkin, 2006, Stefanovsky et al., 2017b]. A few GC studies have been conducted in the last few years targeting this phase. Notably, pyrochlore phase $Ln_2Ti_2O_7$ can convert into a $(Ln_{0.5}U_{0.5})Ti_2O_6$ brannerite phase when uranium is substituted in the system [Zhang et al., 2017b]. Here glass precursor of the composition $Na_2AlBSi_6O_{16}$ is pre-made at low temperature and mixed with a ceramic precursor powder made from calcined alkoxides and nitrates of Ti, Ca, Y/Ce/Eu/Gd/Tb/Dy, and U; these components were then mixed and heat treated at 1200 °C, then slow cooled [Zhang et al., 2018, 2017b, 2019]. When rare earths are also incorporated, most of the U is present as U^{5+} for charge compensation, and in cerium-containing compositions the Ce is mostly Ce^{3+} [Zhang et al., 2018]. More recent studies used cold-press and sinter at 1200 °C from the same glass precursor $Na_2AlBSi_6O_{16}$ but adding oxides TiO_2 and UO_2 in different ratios [Dixon Wilkins et al., 2020]. GCs were observed, with some TiO_2 dissolving into the glass phase and preventing the desired brannerite unless excess TiO_2 was added. In this study, brannerite was suggested to form around starting UO_2 particles until they were consumed or the kinetic barrier prevented diffusion; this barrier was thought to be lower for brannerite GC than for brannerite ceramics [Dixon Wilkins et al., 2020].

4.4.4. *Phosphates*

In the phosphate family of mineral and related synthetic phases [Ewing and Wang, 2002], the main considered phases have been phosphate apatite (e.g. $Ca_8Nd_2(PO_4)_6O_2$ or $Ca_5(PO_4)_3F$), monazite ($CePO_4$)/xenotime (YPO_4), vitusite ($Na_3Ce(PO_4)_2$), and synthetic phases related to kosnarite ($KZr_2(PO_4)_3$) such as $NaZr_2(PO_4)_3$ (NZP) and $Zr_2(PO_4)_3$ [Roy et al., 1982].

Phosphate **apatite** phases have been targeted for wastes containing high amounts of halides. GCs made with waste calcine from the Idaho Chemical Processing plant, rich in Al_2O_3, B_2O_3, ZrO_2, CaF_2, Na_2O, CaO, and CdO, were designed with added SiO_2, MgO, and P_2O_5 [Raman, 1998]. The waste calcine plus additives was HIP in stainless steel canisters at 138 MPa and 1000 °C, producing a GC with multiple ceramic phases, including several containing Zr or Ca, including $Ca_5(PO_4)_3F$ fluoro-apatite. This study [Raman, 1998] is a good example of designing the additives to produce a set of targeted crystalline phases. Recently fluorapatite phases have been created by two-step sintering of iron phosphate glass with SrF_2, in an effort to explore waste forms for immobilizing the halides in molten salt reactors [Zhou et al., 2021]; other researchers, however, have emphasized the low waste loading of fluorine in this scheme [Gregg et al., 2020b]. GC for dental applications have been demonstrated from phosphate glasses with Sr phosphates and Sr- and Ca-fluorapatite plus xenotime and monazite [Ritzberger et al., 2013] or with chlorapatite from aluminosilicate glasses [Chen et al., 2014].

In recent years, more focus has been given to **monazite**-based GC systems. Monazite is a very flexible structure which in nature is based on phosphate but can form in other chemistries, and can incorporate a wide variety of metal ions [Clavier and Dacheux, 2011, Montel, 2011]. In one example, a lanthanum metaphosphate glass powder is mixed with simulated HLW calcine (Nd^{3+} and Zr^{4+} used to simulate transuranics, plus La, Ce, Fe, and Mo) and heated to 1200 °C then cooled in the unpowered furnace, producing monazite and ZrP_2O_7 crystals in glass [He et al., 2008].

Given the desirable chemical durability properties of iron phosphate glasses [Joseph et al., 2017], a number of studies have looked at crystallization from this base glass type, sometimes including B_2O_3 or TiO_2 to suppress unwanted crystalline phases like ZrP_2O_7 or $FePO_4$ [Asuvathraman et al., 2015, Deng et al., 2018, Wang et al., 2016, 2020b]. The main phase produced is monazite, which ends up as a mixed phase such as $(Ce,La,Nd)PO_4$ depending on the lanthanides added [Deng et al., 2018, Wang et al., 2016, 2020b,c].

Much less research has been conducted on phosphate GC based on NZP-type phases or **vitusite**.

GCs based on NZP have been recently demonstrated, using an iron borophosphate base glass with added Na_2O and ZrO_2 [Liu et al., 2019, Wang et al., 2020a]. Though these initial studies have not shown incorporation of target waste ions, in theory NZP could accommodate Sr, Cs, and actinides in its structure [Ewing and Wang, 2002]. Vitusite GC were investigated to immobilize lanthanide fission product wastes produced during pyro-processing of used uranium fuel, where the lanthanide oxides were mixed with borosilicate glass with P_2O_5 to facilitate formation of the desired $Na_3Ln(PO_4)_2$ vitusite phase, which was shown to sequester Ce and Nd [Kim and Heo, 2015]. A subsequent structural study showed that the vitusite phase, because it requires Na for formation, can closely sequester Nd and also improve the chemical durability, with respect to Na, compared to the uncrystallized glass [Kim et al., 2017].

4.4.5. *Cs/Sr/Ba waste forms*

In early studies of nuclear waste immobilization, it was recognized that waste forms would be needed for the highly radioactive and short half-life nuclides of Cs, Sr, and Ba. To immobilize Ba, extensive proof-of-concept studies were made of GCs based on **celsian** ($BaAl_2Si_2O_8$) and on **fresnoite** ($Ba_2TiSi_2O_8$), first developed in Germany [Hayward, 1988a, Lutze et al., 1979]. Celsian ceramics and GC are used for various technological applications including dielectrics, insulators, and low expansion materials [Lee et al., 1995]. Similarly, fresnoite GC has been extensively studied for technological applications such as piezoelectrics and nonlinear optics and also for fundamental understanding of isochemical crystallization [Wisniewski et al., 2018].

On further study, fresnoite GCs were found to be of higher durability due to the boron-rich glass phase required for producing celsian GCs [Hayward, 1988a]. Other phases considered for Ba and Sr were scheelite/powellite ($BaMoO_4$) [Hayward, 1988a], and it has been confirmed recently that when combined with Ca will form two molybdate phases in nuclear GC, one containing Ca and Sr, the other Ba and Sr [Crum et al., 2014]. Celsian systems studied formed celsian (monoclinic or hexagonal), titanate pyrochlore, scheelite, pollucite ($CsAlSi_2O_6$), and rarely Mo-nosean ($Na_8AlMoO_4(SiO_4)_6$). Both celsian and pollucite have been seen as minor phases in US GC systems mentioned above where the primary crystalline phases are oxyapatite and powellite [Kissinger et al., 2021, Tang et al., 2014]. In fresnoite GC, the main phases are scheelite, titanate pyrochlore, fresnoite, and Ba-priderite (a hollandite structure phase $BaFe_2Ti_6O_{16}$ [Lee et al., 2006]) with Cs staying in the residual glassy phase.

The mineral **hollandite** is $Ba(Mn^{4+})_6(Mn^{3+})_2O_{16}$, but this structure is very flexible and offers substitution for Cs and Ba in the channels of the $(Ti,Al)O_6$ rings, which substitute for the MnO_6 rings in the phases of interest [Ringwood et al., 1979b]. Hollandite has also been envisaged as a phase for immobilization of Cs, being stable under beta and gamma irradiation [Caurant et al., 2007a], but possibly only for ceramic waste forms. Hollandite phases for ceramic nuclear waste forms have been well-studied for nuclear waste [Caurant, 2014, Chen et al., 2016, Hyatt et al., 2011, Xu et al., 2015a] and hazardous waste [Krausova et al., 2016] immobilization of large univalent and divalent (e.g., Ba^{2+}, Cd^{2+}, Pb^{2+}) ions.

Another possible phase for immobilizing Cs, as well as minor Rb, is **pollucite** ($CsAlSi_2O_6$) [Crum et al., 2012, Tang et al., 2014]. GCs with the pollucite phase have been reported starting with SiO_2–Al_2O_3–Cs_2O glass, with pollucite crystals and mullite ($Al_6Si_2O_{13}$) forming with residual glass on heat treatment [Caurant et al., 2007a]. As mentioned above, pollucite phases were observed in celsian GC [Hayward, 1988a]. Attempts to produce designed glasses to crystallize pollucite failed due to the excessive temperatures needed and lack of nucleation [Strachan and Schultz, 1976].

Recently, there has been increased interest in developing pollucite GC for immobilizing Cs-contaminated soil, such as that at the Fukushima nuclear accident site in Japan. In one recent study, a Na_2O–CaO alumino-boro-silicate glass frit was mixed with a Cs silicate and melted to form glass which crystallized pollucite on heat treatment [Yang et al., 2021]. Another study used a geopolymer process to produce alkali activated solution (CsOH, NaOH) with colloidal silica, which was then mixed with metakaolin (Al, Si source) and B_2O_3 then heat treated >700 °C to crystallize pollucite [He et al., 2020]. If higher conversion temperatures are used for the geopolymer, Cs is volatilized and crystalline phases tend toward Cs-substituted leucite (feldspar, nominally $KAlSi_2O_6$) and $CsAl_2Si_5O_{12}$ [Chen et al., 2019b].

Other demonstrations have focused on directly converting inorganic ion exchange media designed to remove Cs. In one study, crystalline silicotitanate (CST) ion exchange media (which also contains Nb and a Zr-hydroxide binder) was used to separate Cs-contaminated water. HIP of these Cs-exchanged media form $CsTiNb_6O_{18}$ (a pyrochlore analogue [Chen et al., 2016]) and $Cs_2ZrSi_6O_{15}$ plus mixed (Ti,Zr,Nb) dioxides and other minor phases of zircon and $NaNbO_3$ [Chen et al., 2018]. In another study, chabazite-zeolite-containing Cs was HIPped creating Cs-substituted leucite and residual glass along with other feldspars albite and anorthite and minor diopside [Gardner et al., 2021].

5. Conclusions

In the current review, we summarize some of the important issues surrounding vitrification of industrial and nuclear wastes, with an emphasis on the importance of waste component solubility and resulting undesired crystallization, compared with the deliberate design for the crystallization and production of GCs. Throughout, we compare the level of industrialization for waste forms, which is generally quite advanced for glasses but relatively immature for GCs. Waste glass vitrification using both hot crucible induction melters and joule-heated ceramic melters are relatively mature technologies and have been immobilizing nuclear waste for decades, for both commercial fuel reprocessing wastes and for legacy defense wastes. Despite this level of international experience, idiosyncrasies with waste composition in particular countries due to specific processing paths or storage histories require novel designs for efficient and safe vitrification of a durable vitreous waste form.

We emphasize some of the considerations and challenges for immobilizing certain waste streams, and summarize recent developments especially in several important GC systems, where the target crystalline phases are phosphates, silicates, zirconates, or titanates. Some aspects of crystal chemistry of these phases is offered to help with design of GCs to immobilize particular waste components. A large amount of recent GC work has focused on new waste streams, such as those coming from nuclear accidents and containing large amounts of highly radioactive heavy alkali and alkaline-earth metals (Cs, Sr, Ba). Other recent efforts have focused on novel processing methods, such as HIP to incorporate plutonium into zirconolite while maintained in a borosilicate matrix, or cold crucible induction melting allowing both high temperature melting and nucleation and growth on cooling.

Conflicts of interest

Authors have no conflict of interest to declare.

Acknowledgments

JSM thanks the United States Department of Energy (US DOE) Waste Treatment & Immobilization Plant (WTP) Federal Project Office for funding, under the direction of Dr. Albert A. Kruger, contract number 89304017CEM000001. JSM also gratefully acknowledges support from the US–UK Fulbright Commission for support during his sabbatical in 2019 which focused on international issues surrounding nuclear waste management. The authors also thank Daniel Neuville for the invitation to write this review. SSC gratefully acknowledges CEA, ORANO and EDF for support and cooperation.

References

Aleshin, E. and Roy, R. (1962). Crystal chemistry of pyrochlore. *J. Am. Ceram. Soc.*, 45, 18–25.

Alton, J., Plaisted, T. J., and Hrma, P. (2002a). Kinetics of growth of spinel crystals in a borosilicate glass. *Chem. Eng. Sci.*, 57, 2503–2509.

Alton, J., Plaisted, T. J., and Hrma, P. (2002b). Dissolution and growth of spinel crystals in a borosilicate glass. *J. Non-Cryst. Solids*, 311, 24–35.

Amoroso, J. W., Marra, J., Dandeneau, C. S., Brinkman, K., Xu, Y., Tang, M., Maio, V., Webb, S. M., and Chiu, W. K. S. (2017). Cold crucible induction melter test for crystalline ceramic waste form fabrication: A feasibility assessment. *J. Nucl. Mater.*, 486, 283–297.

Asmussen, R. M., Neeway, J. J., Kaspar, T. C., and Crum, J. V. (2017). Corrosion behavior and microstructure influence of glass-ceramic nuclear waste forms. *Corrosion*, 73, 1306–1319.

Asuvathraman, R., Joseph, K., Raja Madhavan, R., Sudha, R., Krishna Prabhu, R., and Govindan Kutty,

K. V. (2015). A versatile monazite–IPG glass–ceramic waste form with simulated HLW: Synthesis and characterization. *J. Eur. Ceram. Soc.*, 35, 4233–4239.

Bardez-Giboire, I., Kidari, A., Magnin, M., Dussossoy, J.-L., Peuget, S., Caraballo, R., Tribet, M., Doreau, F., and Jégou, C. (2017). Americium and trivalent Lanthanides incorporation in high-level waste glass-ceramics. *J. Nucl. Mater.*, 492, 231–238.

Bart, F., L'Hermite, V., Houpert, S., Fillet, C., Pacaud, F., and Jacquet-Francillon, N. (1998). Development of apatite-based glass ceramics for actinide immobilization. *Ceram. Trans.*, 87, 511–520.

Billings, A. L. and Fox, K. M. (2010). Retention of sulfate in savannah river site high-level radioactive waste glass. *Int. J. Appl. Glass Sci.*, 1, 388–400.

Bingham, P. A., Vaishnav, S., Forder, S. D., Scrimshire, A., Jaganathan, B., Rohini, J., Marra, J. C., Fox, K. M., Pierce, E. M., Workman, P., and Vienna, J. D. (2017). Modelling the sulfate capacity of simulated radioactive waste borosilicate glasses. *J. Alloys Compd.*, 695, 656–667.

Blackburn, L. R., Bailey, D. J., Sun, S.-K., Gardner, L. J., Stennett, M. C., Corkhill, C. L., and Hyatt, N. C. (2021). Review of zirconolite crystal chemistry and aqueous durability. *Adv. Appl. Ceram.*, pages 1–15.

Blackburn, L. R. and Hyatt, N. C. (2021). Actinide immobilization in dedicated wasteforms: An alternative pathway for the long-term management of existing actinide stockpiles. In Greenspan, E., editor, *Encyclopedia of Nuclear Energy*, pages 650–662. Elsevier, Oxford.

Boccaccini, A. R., Atiq, S., and Grimes, R. W. (2003). Hot-pressed glass matrix composites containing pyrochlore phase particles for nuclear waste encapsulation. *Adv. Eng. Mater.*, 5, 501–508.

Boccaccini, A. R., Bernardo, E., Blain, L., and Boccaccini, D. N. (2004). Borosilicate and lead silicate glass matrix composites containing pyrochlore phases for nuclear waste encapsulation. *J. Nucl. Mater.*, 327, 148–158.

Boué, E., Schuller, S., Toplis, M. J., Charpentier, T., Mesbah, A., Pablo, H., Monnereau, M., and Moskura, M. (2019). Kinetic and thermodynamic factors controlling the dissolution of molybdate-bearing calcines during nuclear glass synthesis. *J. Nucl. Mater.*, 519, 74–87.

Brehault, A., Patil, D., Kamat, H., Youngman, R. E., Thirion, L. M., Mauro, J. C., Corkhill, C. L., McCloy, J. S., and Goel, A. (2018). Compositional dependence of solubility/retention of molybdenum oxides in aluminoborosilicate-based model nuclear waste glasses. *J. Phys. Chem. B*, 122, 1714–1729.

Brinkman, K., Fox, K., Marra, J., Reppert, J., Crum, J., and Tang, M. (2013). Single phase melt processed powellite (Ba,Ca)MoO_4 for the immobilization of Mo-rich nuclear waste. *J. Alloys Compd.*, 551, 136–142.

Brow, R. K., Kim, C. W., and Reis, S. T. (2020). Iron polyphosphate glasses for waste immobilization. *Int. J. Appl. Glass Sci.*, 11, 4–14.

Buykx, W. J., Levins, D. M., Smart, R. S. C., Smith, K. L., Stevens, G. T., Watson, K. G., and White, T. J. (1990). Processing impurities as phase assemblage modifiers in titanate nuclear waste ceramics. *J. Am. Ceram. Soc.*, 73, 217–225.

Carter, M. L., Li, H., Zhang, Y., Gillen, A. L., and Vance, E. R. (2009). HIPed tailored pyrochlore-rich glass-ceramic waste forms for the immobilization of nuclear waste. *Proc. MRS*, 1124, article no. 401.

Carter, M. L., Stewart, M. W. A., Leung, S. H. F., Colella, M., and Vance, E. R. (1996). Microstructures of inactive synroc-C samples produced by different hot-consolidation methods. *Ceram. Trans.*, 71, 491–504.

Casler, D. G. and Hrma, P. (1999). Nonisothermal kinetics of spinel crystallization in a HLW glass. *Proc. MRS*, 556, article no. 255.

Caurant, D. (2014). Spectroscopic investigations on glasses, glass-ceramics and ceramics developed for nuclear waste immobilization. *Opt. Spectrosc.*, 116, 667–676.

Caurant, D. (2017). Glass-ceramics for waste immobilization. In Neuville, D., Cormier, L., Caurant, D., and Montagne, L., editors, *From Glass to Crystal – Nucleation, Growth and Phase Separation: from Research to Applications*, pages 492–525. EDP Sciences, Les Ulis, France.

Caurant, D., Loiseau, P., Aubin-Chevaldonnet, V., Gourier, D., Majérus, O., and Bardez-Giboire, I. (2007a). Studies on ceramics and glass-ceramics for immobilization of high-level nuclear wastes. In Keister, J. E., editor, *Nuclear Materials Research Developments*, pages 1–138. Nova, New York.

Caurant, D., Loiseau, P., Bardez, I., and Gervais, C. (2007b). Effect of Al_2O_3 concentration on zirconolite (Ca(Zr,Hf)Ti_2O_7) crystallization in (TiO_2,ZrO_2,HfO_2)-rich SiO_2–Al_2O_3–CaO–Na_2O

glasses. *J. Mater. Sci.*, 42, 8558–8570.

Caurant, D., Loiseau, P., Majerus, O., Aubin-Chevaldonnet, V., Bardez, I., and Quintas, A. (2009). *Glasses, Glass-Ceramics and Ceramics for Immobilization of Highly Radioactive Nuclear Wastes.* Nova Science Publishers, Inc., New York.

Caurant, D. and Majérus, O. (2021). *Glasses and Glass-Ceramics for Nuclear Waste Immobilization. Reference Module in Materials Science and Materials Engineering.* Elsevier, Oxford.

Caurant, D., Majérus, O., Fadel, E., Quintas, A., Gervais, C., Charpentier, T., and Neuville, D. (2010). Structural investigations of borosilicate glasses containing MoO_3 by MAS NMR and Raman spectroscopies. *J. Nucl. Mater.*, 396, 94–101.

Caurant, D., Majerus, O., Loiseau, P., Bardez, I., Baffier, N., and Dussossoy, J. L. (2006). Crystallization of neodymium-rich phases in silicate glasses developed for nuclear waste immobilization. *J. Nucl. Mater.*, 354, 143–162.

Chen, H., Li, B., Zhao, M., Zhang, X., Du, Y., Shi, Y., and McCloy, J. S. (2019a). Lanthanum modification of crystalline phases and residual glass in augite glass ceramics produced with industrial solid wastes. *J. Non-Cryst. Solids*, 524, article no. 119638.

Chen, H., Marcial, J., Ahmadzadeh, M., Patil, D., and McCloy, J. (2020). Partitioning of rare earths in multiphase nuclear waste glass-ceramics. *Int. J. Appl. Glass Sci.*, 11, 660–675.

Chen, S., Ren, D., Liu, L.-K., Luo, J., and Yang, G.-L. (2019b). Sintering of metakaolin-based Na/Ca-geopolymers and their immobilization of Cs. *J. Am. Ceram. Soc.*, 102, 7125–7136.

Chen, T.-Y., Maddrell, E. R., Hyatt, N. C., Gandy, A. S., Stennett, M. C., and Hriljac, J. A. (2018). Transformation of Cs-IONSIV® into a ceramic wasteform by hot isostatic pressing. *J. Nucl. Mater.*, 498, 33–43.

Chen, T.-Y., Maddrell, E. R., Hyatt, N. C., and Hriljac, J. A. (2016). A potential wasteform for Cs immobilization: synthesis, structure determination, and aqueous durability of $Cs_2TiNb_6O_{18}$. *Inorg. Chem.*, 55, 12686–12695.

Chen, X., Hill, R., and Karpukhina, N. (2014). Chlorapatite glass-ceramics. *Int. J. Appl. Glass Sci.*, 5, 207–216.

Chong, S., Riley, B. J., and Nelson, Z. J. (2021). Crystalline compounds for remediation of rare-earth fission products: A review. *J. Rare Earths.* (in press).

Chouard, N., Caurant, D., Majérus, O., Dussossoy, J. L., Loiseau, P., Grygiel, C., and Peuget, S. (2019). External irradiation with heavy ions of neodymium silicate apatite ceramics and glass-ceramics. *J. Nucl. Mater.*, 516, 11–29.

Chouard, N., Caurant, D., Majérus, O., Guezi-Hasni, N., Dussossoy, J.-L., Baddour-Hadjean, R., and Pereira-Ramos, J.-P. (2016). Thermal stability of SiO_2–B_2O_3–Al_2O_3–Na_2O–CaO glasses with high Nd_2O_3 and MoO_3 concentrations. *J. Alloys Compd.*, 671, 84–99.

Clavier, N. and Dacheux, N. (2011). Crystal chemistry of the monazite structure. *J. Eur. Ceram. Soc.*, 31, 941–976.

Crum, J., Maio, V., McCloy, J., Scott, C., Riley, B., Benefiel, B., Vienna, J., Archibald, K., Rodriguez, C., Rutledge, V., Zhu, Z., Ryan, J., and Olszta, M. (2014). Cold crucible induction melter studies for making glass ceramic waste forms: A feasibility assessment. *J. Nucl. Mater.*, 444, 481–492.

Crum, J. V., Neeway, J. J., Riley, B. J., Zhu, Z., Olszta, M. J., and Tang, M. (2016). Dilute condition corrosion behavior of glass-ceramic waste form. *J. Nucl. Mater.*, 482, 1–11.

Crum, J. V., Turo, L., Riley, B., Tang, M., and Kossoy, A. (2012). Multi-phase glass-ceramics as a waste form for combined fission products: Alkalis, alkaline earths, lanthanides, and transition metals. *J. Am. Ceram. Soc.*, 95, 1297–1303.

Deng, Y., Liao, Q., Wang, F., and Zhu, H. (2018). Synthesis and characterization of cerium containing iron phosphate based glass-ceramics. *J. Nucl. Mater.*, 499, 410–418.

Deschanels, X., Lopez, C., Denauwer, C., and Bart, J. M. (2003). Solubility of plutonium and surrogates in nuclear glass matrices. *AIP Conf. Proc.*, 673, 59–60.

Deshkar, A., Gulbiten, O., Youngman, R. E., Mauro, J. C., and Goel, A. (2020). Why does B_2O_3 suppress nepheline ($NaAlSiO_4$) crystallization in sodium aluminosilicate glasses? *Phys. Chem. Chem. Phys.*, 22, 8679–8698.

Deubener, J., Allix, M., Davis, M. J., Duran, A., Höche, T., Honma, T., Komatsu, T., Krüger, S., Mitra, I., Müller, R., Nakane, S., Pascual, M. J., Schmelzer, J. W. P., Zanotto, E. D., and Zhou, S. (2018). Updated definition of glass-ceramics. *J. Non-Cryst. Solids*, 501, 3–10.

Didierlaurent, R., Hugon, I., Lemonnier, S., Girold, C., Prevost, T., Maneglia, F., and David, L. (2019). Applicability evaluation of the In-Can vitrification process to Fukushima waste. In *Proceedings of the 27th International Conference on Nuclear Engineering (ICONE27)*, volume 27, page 1250, Ibaraki, Japan.

Didierlaurent, R., Orefice, H., Turc, H.-A., Hollebecque, J.-F., Fournier, M., Shibata, K., and David, L. (2020). DEM and MELT In-Can vitrification process for Fukushima Daiichi water treatment secondary waste – 20034. In *WM2020: 46 Annual Waste Management Conference, United States*, Phoenis, USA.

Digeos, A. A., Valdez, J. A., Sickafus, K. E., Atiq, S., Grimes, R. W., and Boccaccini, A. R. (2003). Glass matrix/pyrochlore phase composites for nuclear wastes encapsulation. *J. Mater. Sci.*, 38, 1597–1604.

Dixon Wilkins, M. C., Stennett, M. C., Maddrell, E., and Hyatt, N. C. (2020). The formation of stoichiometric uranium brannerite (UTi_2O_6) glass-ceramic composites from the component oxides in a one-pot synthesis. *J. Nucl. Mater.*, 542, article no. 152516.

Donald, I. W. (2007). Immobilisation of radioactive and non-radioactive wastes in glass-based systems: an overview. *Glass Technol.*, 48, 155–163.

Donald, I. W. (2010). *Waste Immobilization in Glass and Ceramic Based Hosts: Radioactive, Toxic, and Hazardous Wastes*. Wiley, Chichester, West Sussex.

Donald, I. W. (2016). Vitrification of radioactive, toxic and hazardous wastes. In *The Science and Technology of Inorganic Glasses and Glass-Ceramics: From the Ancient to the Present to the Future*, pages 261–300. Society for Glass Technology, Sheffield.

Donald, I. W., Metcalfe, B. L., and Taylor, R. N. J. (1997). The immobilization of high level radioactive wastes using ceramics and glasses. *J. Mater. Sci.*, 32, 5851–5887.

Ebbinghaus, B. (1999). Plutonium immobilization project: baseline formulation. UCRL-ID-113089; PIP-99-012, Lawrence Livermore National Laboratory, Livermore, CA.

Ewing, R. C. (1994). The metamict state: 1993 – the centennial. *Nucl. Instrum. Methods B*, 91, 22–29.

Ewing, R. C. (1999). Nuclear waste forms for actinides. *Proc. Natl. Acad. Sci. USA*, 96, 3432–3439.

Ewing, R. C., Chakoumakos, B. C., Lumpkin, G. R., and Murakami, T. (1987). The metamict state. *MRS Bull.*, 12, 58–66.

Ewing, R. C. and Haaker, R. F. (1980). The metamict state: Implications for radiation damage in crystalline waste forms. *Nucl. Chem. Waste Manag.*, 1, 51–57.

Ewing, R. C., Lutze, W., and Weber, W. J. (1995). Zircon: A host-phase for the disposal of weapons plutonium. *J. Mater. Res.*, 10, 243–246.

Ewing, R. C. and Wang, L. (2002). Phosphates as nuclear waste forms. *Rev. Mineral. Geochem.*, 48, 673–699.

Fahey, J. A., Weber, W. J., and Rotella, F. J. (1985). An X-ray and neutron powder diffraction study of the $Ca_{2+x}Nd_{8-x}(SiO_4)_6O_{2-0.5x}$ system. *J. Solid State Chem.*, 60, 145–158.

Feng, Z., Xie, H., Wang, L., Deng, S., and Li, J. (2019). Glass-ceramics with internally crystallized pyrochlore for the immobilization of uranium wastes. *Ceram. Int.*, 45, 16999–17005.

Fox, K. M., Edwards, T. B., and Peeler, D. K. (2008). Control of nepheline crystallization in nuclear waste glass. *Int. J. Appl. Glass Sci.*, 5, 666–673.

Gardner, L. J., Walling, S. A., Corkhill, C. L., and Hyatt, N. C. (2021). Thermal treatment of Cs-exchanged chabazite by hot isostatic pressing to support decommissioning of Fukushima Daiichi Nuclear Power Plant. *J. Hazard. Mater.*, 413, article no. 125250.

Gin, S., Jollivet, P., Tribet, M., Peuget, S., and Schuller, S. (2017). Radionuclides containment in nuclear glasses: an overview. *Radiochim. Acta*, 105, 927–959.

Glatz, J.-P. (2020). Spent fuel dissolution and reprocessing processes. In Konings, R. J. M. and Stoller, R. E., editors, *Comprehensive Nuclear Materials*, pages 305–326. Elsevier, Oxford, 2nd edition.

Goel, A., McCloy, J. S., Pokorny, R., and Kruger, A. A. (2019). Challenges with vitrification of Hanford high-level waste (HLW) to borosilicate glass – An overview. *J. Non-Cryst. Solids X*, 4, article no. 100033.

Gong, W. L., Lutze, W., and Ewing, R. C. (2000). Zirconia ceramics for excess weapons plutonium waste. *J. Nucl. Mater.*, 277, 239–249.

Green, T. H. and Pearson, N. J. (1987). High-pressure, synthetic loveringite-davidite and its rare earth element geochemistry. *Min. Mag.*, 51, 145–149.

Gregg, D. J., Farzana, R., Dayal, P., Holmes, R., and Triani, G. (2020a). Synroc technology: Perspectives

and current status (Review). *J. Am. Ceram. Soc.*, 103, 5424–5441.

Gregg, D. J., Vance, E. R., Dayal, P., Farzana, R., Aly, Z., Holmes, R., and Triani, G. (2020b). Hot Isostatically Pressed (HIPed) fluorite glass-ceramic wasteforms for fluoride molten salt wastes. *J. Am. Ceram. Soc.*, 103, 5454–5469.

Guillen, D. P., Abboud, A. W., and Fox, K. (2019). Particle settling in a simulated melter discharge riser. *Mater. Lett.*, 236, 38–41.

Gutzow, I. (1980a). Induced crystallization of glass-forming systems: A case of transient heterogeneous nucleation (part II). *Contemp. Phys.*, 21, 243–263.

Gutzow, I. (1980b). Induced crystallization of glass-forming systems: A case of transient heterogeneous nucleation, part 1. *Contemp. Phys.*, 21, 121–137.

Harrison, M. T. (2014). Vitrification of high level waste in the UK. *Proc. Mater. Sci.*, 7, 10–15.

Hayward, P. J. (1988a). Glass-ceramics. In Lutze, W. and Ewing, R. C., editors, *Radioactive Waste Forms for the Future*, pages 427–493. North-Holland, UK.

Hayward, P. J. (1988b). The use of glass ceramics for immobilising high level wastes from nuclear fuel recycling. *Glass Technol.*, 29, 122–136.

He, P., Fu, S., Wang, M., Duan, X., Wang, Q., Li, D., Yang, Z., Jia, D., and Zhou, Y. (2020). B_2O_3-assisted low-temperature crystallization of pollucite structures and their potential applications in Cs+ immobilization. *J. Nucl. Mater.*, 540, article no. 152314.

He, Y., Lü, Y., and Zhang, Q. (2008). Characterization of monazite glass–ceramics as wasteform for simulated α-HLLW. *J. Nucl. Mater.*, 376, 201–206.

Hixson, A. W. and Crowell, J. H. (1931). Dependence of reaction velocity upon surface and agitation. *Ind. Eng. Chem.*, 23, 923–931.

Höche, T., Patzig, C., Gemming, T., Wurth, R., Rüssel, C., and Avramov, I. (2012). Temporal evolution of diffusion barriers surrounding $ZrTiO_4$ nuclei in lithia aluminosilicate glass-ceramics. *Cryst. Growth Des.*, 12, 1556–1563.

Holland, W. and Beall, G. H. (2012). *Glass Ceramic Technology*. Wiley, Westerville, OH, USA.

Hrma, P. (2010). Crystallization during processing of nuclear waste glass. *J. Non-Cryst. Solids*, 356, 3019–3025.

Hrma, P. and Marcial, J. (2011). Dissolution retardation of solid silica during glass-batch melting. *J. Non-Cryst. Solids*, 357, 2954–2959.

Hrma, P., Marcial, J., Swearingen, K. J., Henager, S. H., Schweiger, M. J., and TeGrotenhuis, N. E. (2011). Conversion of batch to molten glass, II: Dissolution of quartz particles. *J. Non-Cryst. Solids*, 357, 820–828.

Hrma, P., Riley, B. J., Crum, J. V., and Matyas, J. (2014). The effect of high-level waste glass composition on spinel liquidus temperature. *J. Non-Cryst. Solids*, 384, 32–40.

Hyatt, N. C. (2017). Plutonium management policy in the United Kingdom: The need for a dual track strategy. *Energy Policy*, 101, 303–309.

Hyatt, N. C., Stennett, M. C., Fiddy, S. G., Wellings, J. S., Dutton, S. S., Maddrell, E. R., Connelly, A. J., and Lee, W. E. (2011). Synthesis and characterisation of transition metal substituted barium hollandite ceramics. *Proc. MRS*, 932, article no. 601.

Isa, H. (2011). A review of glass-ceramics production from silicate wastes. *Int. J. Phys. Sci.*, 6, 6781–6790.

Izak, P., Hrma, P. R., Arey, B. W., and Plaisted, T. J. (2001). Effect of feed melting, temperature history and minor component addition on spinel crystallization in high-level waste glass. *J. Non-Cryst. Solids*, 289, 17–29.

Jantzen, C. M. and Brown, K. G. (2007). Predicting the spinel-nepheline liquidus for application to nuclear waste glass processing. Part I: Primary phase analysis, liquidus measurment, and quasicrystalline approach. *J. Am. Ceram. Soc.*, 90, 1866–1879.

Jantzen, C. M., Imrich, K. J., Brown, K. G., and Pickett, J. B. (2015). High chrome refractory characterization: Part I. Impact of melt reduction/oxidation on the corrosion mechanism. *Int. J. Appl. Glass Sci.*, 6, 137–157.

Jelena, M., Bratislav, T., Martina, G., Milena, M.-C., Katsumi, Y., Anna, G., and Branko, M. (2020). Synthesis and characterization of monophase CaO–TiO_2–SiO_2 (sphene) based glass-ceramics. *Sci. Sin.*, 52, 41–52.

Jiang, W., Kovarik, L., Zhu, Z., Varga, T., Engelhard, M. H., Bowden, M. E., Nenoff, T. M., and Garino, T. J. (2014). Microstructure and Cs behavior of Ba-doped aluminosilicate pollucite irradiated with F+ ions. *J. Phys. Chem. C*, 118, 18160–18169.

Jin, T., Kim, D., Tucker, A. E., Schweiger, M. J., and Kruger, A. A. (2015). Reactions during melting of low-activity waste glasses and their effects

on the retention of rhenium as a surrogate for technetium-99. *J. Non-Cryst. Solids*, 425, 28–45.

Joseph, K., Stennett, M. C., Hyatt, N. C., Asuvathraman, R., Dube, C. L., Gandy, A. S., Govindan Kutty, K. V., Jolley, K., Vasudeva Rao, P. R., and Smith, R. (2017). Iron phosphate glasses: Bulk properties and atomic scale structure. *J. Nucl. Mater.*, 494, 342–353.

Kamat, H. (2021). *Rare-earth oxides in aluminoborosilicate glasses and their impact on molybdenum oxide solubility in nuclear waste glasses*. PhD thesis, The State University of New Jersey, New Brunswick, New Jersey.

Kamat, H., Arias-Serrano, B. I., Yaremchenko, A., and Goel, A. (2020). Ruthenium solubility and its impact on the crystallization behavior and electrical conductivity of MoO_3-containing borosilicate-based model high-level nuclear waste glasses. *J. Non-Cryst. Solids*, 549, article no. 120356.

Kamat, H., Wang, F., Barnsley, K., Hanna, J. V., Tyryshkin, A. M., and Goel, A. (2021). Insight into the partitioning and clustering mechanism of rare-earth cations in alkali aluminoborosilicate glasses.

Karamanov, A. (2009). Granite like materials from hazardous wastes obtained by sintercrystallisation of glass frits. *Adv. Appl. Ceram.*, 108, 14–21.

Karamanov, A., Paunović, P., Ranguelov, B., Ljatifi, E., Kamusheva, A., Načevski, G., Karamanova, E., and Grozdanov, A. (2017). Vitrification of hazardous Fe-Ni wastes into glass-ceramic with fine crystalline structure and elevated exploitation characteristics. *J. Envir. Chem. Eng.*, 5, 432–441.

Kaushik, C. P. (2014). Indian program for vitrification of high level radioactive liquid waste. *Proc. Mater. Sci.*, 7, 16–22.

Kaushik, C. P., Mishra, R. K., Sengupta, P., Kumar, A., Das, D., Kale, G. B., and Raj, K. (2006). Barium borosilicate glass – a potential matrix for immobilization of sulfate bearing high-level radioactive liquid waste. *J. Nucl. Mater.*, 358, 129–138.

Kim, D. and Kruger, A. A. (2018). Volatile species of technetium and rhenium during waste vitrification. *J. Non-Cryst. Solids*, 481, 41–50.

Kim, M. and Heo, J. (2015). Vitusite glass-ceramics wasteforms for immobilization of lanthanide wastes generated by pyro-processing. *Ceram. Int.*, 41, 6132–6136.

Kim, M. A., Song, J. H., Um, W., Hyatt, N., Sun, S.-K., and Heo, J. (2017). Structure analysis of vitusite glass–ceramic waste forms using extended X-ray absorption fine structures. *Ceram. Int.*, 43, 4687–4691.

Kimura, R., Inagaki, Y., Idemitsu, K., and Arima, T. (2018). Vitrification processes of simulated cesium sorbing zeolite waste. *Prog. Nucl. Energy*, 108, 497–502.

Kissinger, R. M., Crum, J. V., and Riley, B. J. (2021). Single-component-at-a-time variation study for glass-ceramic waste forms. *J. Am. Ceram. Soc.*, 104, 3738–3749.

Kong, L., Karatchevtseva, I., Chironi, I., Wei, T., and Zhang, Y. (2019). $CaZrTi_2O_7$ zirconolite synthesis: from ceramic to glass-ceramic. *Int. J. Appl. Glass Sci.*, 16, 1460–1470.

Kong, L., Karatchevtseva, I., and Zhang, Y. (2017a). A new method for production of glass-$Ln_2Ti_2O_7$ pyrochlore (Ln = Gd, Tb, Er, Yb). *J. Eur. Ceram. Soc.*, 37, 4963–4972.

Kong, L., Zhang, Y., and Karatchevtseva, I. (2017b). Preparation of $Y_2Ti_2O_7$ pyrochlore glass-ceramics as potential waste forms for actinides: The effects of processing conditions. *J. Nucl. Mater.*, 494, 29–36.

Krausova, K., Gautron, L., Karnis, A., Catillon, G., and Borensztajn, S. (2016). Glass ceramics and mineral materials for the immobilization of lead and cadmium. *Ceram. Int.*, 42, 8779–8788.

Krishnamurthy, A., Michaelis, V. K., and Kroeker, S. (2021). Network formation in borosilicate glasses with aluminum or gallium: Implications for nepheline crystallization. *J. Phys. Chem. C*, 125, 8815–8824.

Kroeker, S., Schuller, S., Wren, J. E. C., Greer, B. J., and Mesbah, A. (2016). 133Cs and 23Na MAS NMR spectroscopy of molybdate crystallization in model nuclear glasses. *J. Am. Ceram. Soc.*, 99, 1557–1564.

Kruger, A. A., Cooley, S. K., Joseph, I., Pegg, I. L., Piepel, G. F., Gan, H., and Muller, I. (2013). Final Report – ILAW PCT, VHT, Viscosity, and Electrical Conductivity Model Development, p. Medium: ED. ORP-56502; VSL-07R1230-1, Vitreous State Laboratory, Catholic University of America, United States.

Kruger, A. A., Muller, I. S., Joseph, I., Matlack, K. S., Gan, H., and Pegg, I. L. (2010). *Waste Loading Enhancements for Hanford Law Glasses*. Final Report VSL-10R1790-1. Vitreous State Laboratory, the Catholic University Of America, Washington, DC.

Laverov, N. P., Omel'yanenko, B. I., Yudintsev, S. V.,

Stefanovsky, S. V., and Nikonov, B. S. (2013). Glasses for immobilization of low- and intermediate-level radioactive waste. *Geol. Ore Dep.*, 55, 71–95.

Lee, W. E., Chen, M., and James, P. F. (1995). Crystallization of Celsian ($BaAl_2Si_2O_8$) glass. *J. Am. Ceram. Soc.*, 78, 2180–2186.

Lee, W. E., Ojovan, M. I., and Jantzen, C. M. (2013). *Radioactive Waste Management and Contaminated Site Clean-Up: Processes, Technologies and International Experience*. Woodhead Publishing Series in Energy, 48. Woodhead Publishing, Oxford.

Lee, W. E., Ojovan, M. I., Stennett, M. C., and Hyatt, N. C. (2006). Immobilisation of radioactive waste in glasses, glass composite materials and ceramics. *Adv. Appl. Ceram.*, 105, 3–12.

Lei, J., Wang, B., Xu, L., Teng, Y., Li, Y., Deng, H., and Wu, L. (2021). Role of $Ba(NO_3)$ pretreatment in reducing the yellow phase formation during vitrification of nuclear waste. *J. Nucl. Mater.*, 555, article no. 153121.

Lenoir, M., Grandjean, A., Poissonnet, S., and Neuville, D. R. (2009). Quantitation of sulfate solubility in borosilicate glasses using Raman spectroscopy. *J. Non-Cryst. Solids*, 355, 1468–1473.

Li, H., Hrma, P., Vienna, J. D., Qian, M., Su, Y., and Smith, D. E. (2003). Effects of Al_2O_3, B_2O_3, Na_2O, and SiO_2 on nepheline formation in borosilicate glasses: chemical and physical correlations. *J. Non-Cryst. Solids*, 331, 202–216.

Li, H., Vienna, J. D., Hrma, P., Smith, D. E., and Schweiger, M. J. (1997). Nepheline precipitation in high-level waste glasses: Compositional effects and impact on the waste form acceptability. In *Materials Research Society Symposium – Proceedings*, volume 465, pages 261–268, USA.

Li, H., Wu, L., Xu, D., Wang, X., Teng, Y., and Li, Y. (2015). Structure and chemical durability of barium borosilicate glass–ceramics containing zirconolite and titanite crystalline phases. *J. Nucl. Mater.*, 466, 484–490.

Li, J., Wang, M., and Lu, P. (2021). Nucleating role of P_2O_5 in nepheline-based transparent glass-ceramics. *J. Am. Ceram. Soc.*, 104, 5614–5624.

Liao, C.-Z., Liu, C., Lee, P.-H., Stennett, M. C., Hyatt, N. C., and Shih, K. (2017). Combined quantitative X-ray diffraction, scanning electron microscopy, and transmission electron microscopy investigations of crystal evolution in CaO–Al_2O_3–SiO_2–TiO_2–ZrO_2–Nd_2O_3–Na_2O System. *Cryst. Growth Des.*, 17, 1079–1087.

Liu, J., Wang, F., Liao, Q., Zhu, H., Liu, D., and Zhu, Y. (2019). Synthesis and characterization of phosphate-based glass-ceramics for nuclear waste immobilization: Structure, thermal behavior, and chemical stability. *J. Nucl. Mater.*, 513, 251–259.

Ljatifi, E., Kamusheva, A., Grozdanov, A., Paunović, P., and Karamanov, A. (2015). Optimal thermal cycle for production of glass–ceramic based on wastes from ferronickel manufacture. *Ceram. Int.*, 41, 11379–11386.

Loiseau, P. and Caurant, D. (2010). Glass–ceramic nuclear waste forms obtained by crystallization of SiO_2–Al_2O_3–CaO–ZrO_2–TiO_2 glasses containing lanthanides (Ce, Nd, Eu, Gd, Yb) and actinides (Th): Study of the crystallization from the surface. *J. Nucl. Mater.*, 402, 38–54.

Loiseau, P., Caurant, D., Majerus, O., Baffier, N., and Fillet, C. (2003a). Crystallization study of (TiO_2, ZrO_2)-rich SiO_2–Al_2O_3–CaO glasses Part I Preparation and characterization of zirconolite-based glass-ceramics. *J. Mater. Sci.*, 38, 843–852.

Loiseau, P., Caurant, D., Majerus, O., Baffier, N., and Fillet, C. (2003b). Crystallization study of (TiO_2, ZrO_2)-rich SiO_2–Al_2O_3–CaO glasses Part II Surface and internal crystallization processes investigated by differential thermal analysis (DTA). *J. Mater. Sci.*, 38, 853–864.

Lopez, C., Deschanels, X., Bart, J. M., Boubals, J. M., Den Auwer, C., and Simoni, E. (2003). Solubility of actinide surrogates in nuclear glasses. *J. Nucl. Mater.*, 312, 76–80.

Lopez, C., Deschanels, X., Den Auwer, C., Cachia, J., Bart, J. M., and Peuget, S. (2005). X ray absorption studies of borosilicate glasses containing dissolved actinides or surrogates. *Phys. Scr. T*, 115, 342–345.

Lu, P., Zan, Y., Ren, J., Zhao, T., Xu, K., and Goel, A. (2021). Structure and crystallization behavior of phosphorus-containing nepheline ($NaAlSiO_4$) based sodium aluminosilicate glasses. *J. Non-Cryst. Solids*, 560, article no. 120719.

Lukens, W. W., Magnani, N., Tyliszczak, T., Pearce, C. I., and Shuh, D. K. (2016). Incorporation of technetium into spinel ferrites. *Environ. Sci. Technol.*, 50, 13160–13168.

Luksic, S. A., Riley, B. J., Schweiger, M., and Hrma, P. (2015). Incorporating technetium in minerals and other solids: A review. *J. Nucl. Mater.*, 466, 526–538.

Lumpkin, G. R. (2006). Ceramic waste forms for actinides. *Elements*, 2, 365–372.

Lumpkin, G. R. and Geisler-Wierwille, T. (2012). 5.22 – minerals and natural analogues. In Konings, R. J. M., editor, *Comprehensive Nuclear Materials*, pages 563–600. Elsevier, Oxford.

Lutze, W., Borchardt, J., and De, A. K. (1979). Classification of glass and glass-ceramic nuclear waste forms. In *Scientific Basis for Nuclear Waste Management, I*, pages 69–81. Boston, USA.

Ma, Q., Ding, L., Wang, Q., Yu, Y., Luo, L., and Li, H. (2018). Preparation and characterization of continuous fly ash derived glass fibers with improved tensile strength. *Mater. Lett.*, 231, 119–121.

Maddrell, E., Thornber, S., and Hyatt, N. C. (2015). The influence of glass composition on crystalline phase stability in glass-ceramic wasteforms. *J. Nucl. Mater.*, 456, 461–466.

Maddrell, E. R., Paterson, H. C., May, S. E., and Burns, K. M. (2017). Phase evolution in zirconolite glass-ceramic wasteforms. *J. Nucl. Mater.*, 493, 380–387.

Mahmoudysepehr, M. and Marghussian, V. K. (2009). SiO_2–PbO–CaO–ZrO_2–TiO_2–(B_2O_3–K_2O), a new zirconolite glass–ceramic system: Crystallization behavior and microstructure evaluation. *J. Am. Ceram. Soc.*, 92, 1540–1546.

Manara, D., Grandjean, A., Pinet, O., Dussossoy, J. L., and Neuville, D. R. (2007). Sulfur behavior in silicate glasses and melts: Implications for sulfate incorporation in nuclear waste glasses as a function of alkali cation and V_2O_5 content. *J. Non-Cryst. Solids*, 353, 12–23.

Marcial, J. and McCloy, J. (2019). Role of short range order on crystallization of tectosilicate glasses: A diffraction study. *J. Non-Cryst. Solids*, 505, 131–143.

Marcial, J., Saleh, M., Watson, D., Martin, S. W., Crawford, C. L., and McCloy, J. S. (2019). Boron-speciation and aluminosilicate crystallization in alkali boroaluminosilicate glasses along the $NaAl_{1-x}B_xSiO_4$ and $LiA_{l1-x}B_xSiO_4$ joins. *J. Non-cryst. Solids*, 506, 58–67.

Marples, J. A. C. (1988). The preparation, properties, and disposal of vitrified high level waste from nuclear fuel reprocessing. *Glass Technol.*, 29, 230–247.

Martinez, S., Alfonso, P., de la Fuente, C., and Queralt, I. (1987). Glass ceramic materials from Spanish basalts. In Rincon, J. M., editor, *Glasses and Glass-Ceramics for Nuclear Waste Management*, pages 69–94. Centro de Investigaciones Energeticas Medioambientales y Tecnologicas (CIEMAT) and Instituto de Ceramica y Vidrio, Madrid.

Matyáš, J., Gervasio, V., Sannoh, S. E., and Kruger, A. A. (2017). Predictive modeling of crystal accumulation in high-level waste glass melters processing radioactive waste. *J. Nucl. Mater.*, 495, 322–331.

McClane, D. L., Amoroso, J. W., Fox, K. M., and Kruger, A. A. (2019). Nepheline crystallization behavior in simulated high-level waste glasses. *J. Non-Cryst. Solids*, 505, 215–224.

McClane, D. L., Amoroso, J. W., Hsieh, M. C., Fox, K. M., and Kruger, A. A. (2021). Derivation of the Structural Integrity of Residual (SIR) glass model for the enhancement of waste loading. *J. Am. Ceram. Soc.*, 104, 3235–3246.

McClane, D. L., Fox, K. M., Johnson, F. C., Amoroso, J. W., and Kruger, A. A. (2018). Dissolution of accumulated spinel crystals in simulated nuclear waste glass melts. *J. Hazard. Toxic. Rad. Waste*, 22, article no. 05018001.

McCloy, J. and Goel, A. (2017). Glass-ceramics for nuclear-waste immobilization. *MRS Bull.*, 42, 233–240.

McCloy, J. and Vienna, J. D. (2010). *Glass Composition Constraint Recommendations for Use in Life-Cycle Mission Modeling. PNNL-19372*. Pacific Northwest National Laboratory, Richland, WA.

McCloy, J., Washton, N., Gassman, P., Marcial, J., Weaver, J., and Kukkadapu, R. (2015). Nepheline crystallization in boron-rich alumino-silicate glasses as investigated by multi-nuclear NMR, Raman, & Mössbauer spectroscopies. *J. Non-Cryst. Solids*, 409, 149–165.

McCloy, J. S., Marcial, J., Patil, D., Saleh, M., Ahmadzadeh, M., Chen, H., Crum, J. V., Riley, B. J., Kamat, H., Bréhault, A., Goel, A., Barnsley, K. E., Hanna, J. V., Rajbhandari, P., Corkhill, C. L., Hand, R. J., and Hyatt, N. C. (2019a). Glass structure and crystallization in boro-alumino-silicate glasses containing rare earth and transition metal cations: a US–UK collaborative program. *MRS Adv.*, 4, 1029–1043.

McCloy, J. S., Riley, B. J., Crum, J., Marcial, J., Reiser, J. T., Kruska, K., Peterson, J. A., Neuville, D. R., Patil, D. S., Saleh, M., Barnsley, K. E., and Hanna, J. V. (2019b). Crystallization study of rare earth and molybdenum containing nuclear waste glass ceramics. *J. Am. Ceram. Soc.*, 102, 5149–5163.

McCloy, J. S., Schweiger, M. J., Rodriguez, C. P., and

Vienna, J. D. (2011). Nepheline crystallization in nuclear waste glasses: Progress toward acceptance of high-alumina formulations. *Int. J. Appl. Glass Sci.*, 2, 201–214.

McKeown, D. A., Muller, I. S., Gan, H., Pegg, I. L., and Kendziora, C. A. (2001). Raman studies of sulfur in borosilicate waste glasses: sulfate environments. *J. Non-Cryst. Solids*, 288, 191–199.

McKeown, D. A., Muller, I. S., Gan, H., Pegg, I. L., and Stolte, W. C. (2004). Determination of sulfur environments in borosilicate waste glasses using X-ray absorption near-edge spectroscopy. *J. Non-Cryst. Solids*, 333, 74–84.

McKeown, D. A., Muller, I. S., and Pegg, I. L. (2015). Iodine valence and local environments in borosilicate waste glasses using X-ray absorption spectroscopy. *J. Nucl. Mater.*, 456, 182–191.

Míka, M., Liška, M., and Hrma, P. (2002). The effect of spinel sludge aging on its viscosity. *Ceram. Silikaty*, 46, 148–151.

Mishra, R. K., Sudarsan, K. V., Sengupta, P., Vatsa, R. K., Tyagi, A. K., Kaushik, C. P., Das, D., and Raj, K. (2008). Role of sulfate in structural modifications of sodium barium borosilicate glasses developed for nuclear waste immobilization. *J. Am. Ceram. Soc.*, 91, 3903–3907.

Montel, J.-M. (2011). Minerals and design of new waste forms for conditioning nuclear waste. *Compt. Rend. Geosc.*, 343, 230–236.

Muller, I. S., McKeown, D. A., and Pegg, I. L. (2014). Structural behavior of Tc and I ions in nuclear waste glass. *Proc. Mater. Sci.*, 7, 53–59.

National Research Council, Committee on Waste Forms Technology and Performance (2011). *Waste Forms Technology and Performance: Final Report*. National Academy of Sciences, Washington, DC.

Neeway, J. J., Asmussen, R. M., McElroy, E. M., Peterson, J. A., Riley, B. J., and Crum, J. V. (2018). Kinetics of oxyapatite [$Ca_2Nd_8(SiO_4)6O_2$] and powellite [(Ca,Sr,Ba)MoO_4] dissolution in glass-ceramic nuclear waste forms in acidic, neutral, and alkaline conditions. *J. Nucl. Mater.*, 515, 227–237.

Nucelar Energy Agency (NEA) (2014). Radioactive Waste Management and Decomissioning in the Russian Federation. Radioactive Waste Management Programs in OECD/NEA Member Countries. https://www.oecd-nea.org/rwm/profiles/Russian_Federation_report_web.pdf.

Ojovan, M. and Lee, W. (2011). Glassy wasteforms for nuclear waste immobilization. *Metall. Mat. Trans. A*, 42, 837–851.

Ojovan, M. I., Juoi, J. M., and Lee, W. E. (2008). Application of glass composite materials for nuclear waste immobilization. *J. Pak. Mater. Soc.*, 2, 72–76.

Ojovan, M. I., Petrov, V. A., and Yudintsev, S. V. (2021). Glass crystalline materials as advanced nuclear wasteforms. *Sustainability*, 13, article no. 4117.

Okubo, T. (2018). Current state of efforts at Rokkasho reprocessing plant. *Denki Hyoron*, 103, 40–46.

Omel'yanenko, B. I., Livshits, T. S., Yudintsev, S. V., and Nikonov, B. S. (2007). Natural and artificial minerals as matrices for immobilization of actinides. *Geol. Ore Dep.*, 49, 173–193.

Oniki, T., Tajiri, Y., Mimura, T., Nabemoto, T., and Fukui, T. (2020). Applicability of vitrification technology for secondary waste generated from contaminated water treatment systems at Fukushima Daiichi Nuclear Power Station. *IHI Eng. Rev.*, 53, 1–7.

Pace, S., Cannillo, V., Wu, J., Boccaccini, D. N., Seglem, S., and Boccaccini, A. R. (2005). Processing glass–pyrochlore composites for nuclear waste encapsulation. *J. Nucl. Mater.*, 341, 12–18.

Parkinson, B. G., Holland, D., Smith, M. E., Howes, A. P., and Scales, C. R. (2007). Effect of minor additions on structure and volatilization loss in simulated nuclear borosilicate glasses. *J. Non-Cryst. Solids*, 353, 4076–4083.

Patil, D. S., Konale, M., Gabel, M., Neill, O. K., Crum, J. V., Goel, A., Stennett, M. C., Hyatt, N. C., and McCloy, J. S. (2018). Impact of rare earth ion size on the phase evolution of MoO_3-containing aluminoborosilicate glass-ceramics. *J. Nucl. Mater.*, 510, 539–550.

Pegg, I. L. (2015). Turning nuclear waste into glass. *Phys. Today*, 68, 33–39.

Pegg, I. L., Gan, H., Matlack, K. S., Endo, Y., Fukui, T., Ohashi, A., Joseph, I., and Bowan, B. W. (2010). Mitigation of yellow phase formation at the rokkasho HLW vitrification facility. In *WM-2010 Conference, 2010 March 7–11 Phoenix*, Phoenix, USA.

Peterson, J. A., Crum, J. V., Riley, B. J., Asmussen, R. M., and Neeway, J. J. (2018). Synthesis and characterization of oxyapatite [$Ca_2Nd_8(SiO_4)_6O_2$] and mixed-alkaline-earth powellite [(Ca,Sr,Ba)MoO_4] for a glass-ceramic waste form. *J. Nucl. Mater.*, 510, 623–634.

Pinet, O., Hollebecque, J. F., Hugon, I., Debono, V.,

Campayo, L., Vallat, C., and Lemaitre, V. (2019). Glass ceramic for the vitrification of high level waste with a high molybdenum content. *J. Nucl. Mater.*, 519, 121–127.

Pokorny, R., Rice, J. A., Crum, J. V., Schweiger, M. J., and Hrma, P. (2013). Kinetic model for quartz and spinel dissolution during melting of high-level-waste glass batch. *J. Nucl. Mater.*, 443, 230–235.

Raj, K., Prasad, K. K., and Bansal, N. K. (2006). Radioactive waste management practices in India. *Nucl. Engng Des.*, 236, 914–930.

Raman, S. V. (1998). Microstructures and leach rates of glass–ceramic nuclear waste forms developed by partial vitrification in a hot isostatic press. *J. Mater. Sci.*, 33, 1887–1895.

Raman, S. V. (2000). Properties of metal phosphates and phosphides in glass-ceramic waste forms. *J. Non-Cryst. Solids*, 263–264, 395–408.

Rawlings, R. D., Wu, J. P., and Boccaccini, A. R. (2006). Glass-ceramics: Their production from wastes—A review. *J. Mater. Sci.*, 41, 733–761.

Riley, B. J., McCloy, J. S., Goel, A., Liezers, M., Schweiger, M. J., Liu, J., Rodriguez, C. P., and Kim, D.-S. (2013). Crystallization of rhenium salts in a simulated low-activity waste borosilicate glass. *J. Am. Ceram. Soc.*, 96, 1150–1157.

Riley, B. J., Schweiger, M. J., Kim, D.-S., Lukens, W. W., Williams, B. D., Iovin, C., Rodriguez, C. P., Overman, N. R., Bowden, M. E., Dixon, D. R., Crum, J. V., McCloy, J., and Kruger, A. A. (2014). Iodine solubility in a low-activity waste borosilicate glass at 1000 °C. *J. Nucl. Mater.*, 452, 178–188.

Ringwood, A. E., Kesson, S. E., Reeve, K. D., Levins, D. M., and Ramm, E. J. (1988). Synroc. In Lutze, W. and Ewing, R. C., editors, *Radioactive Waste Forms for the Future*, pages 233–334. Elsevier, Amsterdam, New York.

Ringwood, A. E., Kesson, S. E., Ware, N. G., Hibberson, W., and Major, A. (1979a). Immobilisation of high level nuclear reactor wastes in SYNROC. *Nature*, 278, 219–223.

Ringwood, A. E., Kesson, S. E., Ware, N. G., Hibberson, W. O., and Major, A. (1979b). The SYNROC process: A geochemical approach to nuclear waste immobilization. *Geochem. J.*, 13, 141–165.

Ritzberger, C., Apel, E., Rheinberger, V. M., Schweiger, M., and Höland, W. (2013). Controlled crystallization of xenotime and monazite-type crystals in glass-ceramics. *Phys. Chem. Glasses*, 54, 228–231.

Rose, P. B., Woodward, D. I., Ojovan, M. I., Hyatt, N. C., and Lee, W. E. (2011). Crystallisation of a simulated borosilicate high-level waste glass produced on a full-scale vitrification line. *J. Non-Cryst. Solids*, 357, 2989–3001.

Roy, R., Vance, E. R., and Alamo, J. (1982). [NZP], a new radiophase for ceramic nuclear waste forms. *Mater. Res. Bull.*, 17, 585–589.

Sales, B. C. and Boatner, L. A. (1984). Lead-iron phosphate glass: a stable storage medium for high-level nuclear waste. *Science*, 226, 45–48.

Sargin, I., Lonergan, C. E., Vienna, J. D., McCloy, J. S., and Beckman, S. P. (2020). A data-driven approach for predicting nepheline crystallization in high-level waste glasses. *J. Am. Ceram. Soc.*, 103, 4913–4924.

Scarinci, G., Brusatin, G., Barbieri, L., Corradi, A., Lancellotti, I., Colombo, P., Hreglich, S., and Dall'Igna, R. (2000). Vitrification of industrial and natural wastes with production of glass fibres. *J. Eur. Ceram. Soc.*, 20, 2485–2490.

Schuller, S. (2017). Phase separation in glass. In Neuville, D., Cormier, L., Caurant, D., and Montagne, L., editors, *From Glass to Crystal – Nucleation, Growth and Phase Separation: From Research to Applications*, pages 125–153. EDP Sciences, Les Ulis, France.

Schuller, S., Pinet, O., Grandjean, A., and Blisson, T. (2008). Phase separation and crystallization of borosilicate glass enriched in MoO_3, P_2O_5, ZrO_2, CaO. *J. Non-Cryst. Solids*, 354, 296–300.

Schuller, S., Pinet, O., and Penelon, B. (2011). Liquid–liquid phase separation process in borosilicate liquids enriched in molybdenum and phosphorus oxides. *J. Am. Ceram. Soc.*, 94, 447–454.

Schweiger, M. J., Hrma, P., Humrickhouse, C. J., Marcial, J., Riley, B. J., and TeGrotenhuis, N. E. (2010). Cluster formation of silica particles in glass batches during melting. *J. Non-Cryst. Solids*, 356, 1359–1367.

Sengupta, P., Kaushik, C. P., and Dey, G. K. (2013). Immobilization of high level nuclear wastes: The Indian scenario. In Ramkumar, M., editor, *On a Sustainable Future of the Earth's Natural Resources*, pages 25–51. Springer, Berlin, Heidelberg.

Sheckler, C. A. and Dinger, D. R. (1990). Effect of particle size distribution on the melting of soda–lime–silica glass. *J. Am. Ceram. Soc.*, 73, 24–30.

Short, R. (2014). Phase separation and crystallisation

in UK HLW vitrified products. *Proc. Mater. Sci.*, 7, 93–100.

Singh, B. K., Hafeez, M. A., Kim, H., Hong, S., Kang, J., and Um, W. (2021). Inorganic waste forms for efficient immobilization of radionuclides. *ACS ES&T Eng.*, 1, 1149–1170.

Skidmore, C. H., Vienna, J. D., Jin, T., Kim, D., Stanfill, B. A., Fox, K. M., and Kruger, A. A. (2019). Sulfur solubility in low activity waste glass and its correlation to melter tolerance. *Int. J. Appl. Glass Sci.*, 10, 558–568.

Soderquist, C. Z., Buck, E. C., McCloy, J. S., Schweiger, M. J., and Kruger, A. A. (2016). Formation of technetium salts in hanford low-activity waste glass. *J. Am. Ceram. Soc.*, 99, 3924–3931.

Soderquist, C. Z., Schweiger, M. J., Kim, D.-S., Lukens, W. W., and McCloy, J. S. (2014). Redox-dependent solubility of technetium in low activity waste glass. *J. Nucl. Mater.*, 449, 173–180.

Spasiano, D. and Pirozzi, F. (2017). Treatments of asbestos containing wastes. *J. Envir. Manag.*, 204, 82–91.

Stefanovky, S. V., Yudintsev, S. V., Giere, R., and Lumpkin, G. R. (2004). Nuclear waste form. In Giere, R. and Stille, P., editors, *Energy, Waste and the Environment: A Geological Perspective*, pages 37–63. Geological Society, London.

Stefanovsky, S. V., Stefanovsky, O. I., Danilov, S. S., and Kadyko, M. I. (2019). Phosphate-based glasses and glass ceramics for immobilization of lanthanides and actinides. *Ceram. Int.*, 45, 9331–9338.

Stefanovsky, S. V., Stefanovsky, O. I., Remizov, M. B., Kozlov, P. V., Belanova, E. A., Makarovsky, R. A., and Myasoedov, B. F. (2017a). Sodium–aluminum–iron phosphate glasses as legacy high level waste forms. *Prog. Nucl. Energy*, 94, 229–234.

Stefanovsky, S. V. and Yudintsev, S. V. (2016). Titanates, zirconates, aluminates and ferrites as waste forms for actinide immobilization. *Russ. Chem. Rev.*, 85, 962–994.

Stefanovsky, S. V., Yudintsev, S. V., Shiryaev, A. A., Murzin, V. Y., and Trigub, A. L. (2017b). Phase partitioning and uranium speciation in brannerite-based ceramics. *J. Eur. Ceram. Soc.*, 37, 771–777.

Stefanovsky, S. V., Yudintsev, S. V., Vinokurov, S. E., and Myasoedov, B. F. (2016). Chemical-technological and mineralogical-geochemical aspects of the radioactive waste management. *Geochem. Int.*, 54, 1136–1155.

Stewart, M. W. A., Moricca, S. A., Vance, E. R., Day, R. A., Maddrell, E. R., Scales, C. R., and Hobbs, J. (2013). Hot-isostatic pressing of chlorine-containing plutonium residues and wastes. In *TMS2013 Supplemental Proceedings*, pages 675–682, New York. John Wiley & Sons, Inc.

Strachan, D. and Schultz, W. W. (1976). Glass and ceramic materials for the immobilization of Megacurie-amounts of pure cesium-137. In *Annual Meeting of the American Ceramic Society. ARH-SA-246*, Richland, WA. Atlantic Richfield Hanford Company.

Tang, M., Kossoy, A., Jarvinen, G., Crum, J., Turo, L., Riley, B., Brinkman, K., Fox, K., Amoroso, J., and Marra, J. (2014). Radiation stability test on multiphase glass ceramic and crystalline ceramic waste forms. *Nucl. Instrum. Methods B*, 326, 293–297.

Thornber, S. M., Heath, P. G., Da Costa, G. P., Stennett, M. C., and Hyatt, N. C. (2017). The effect of pre-treatment parameters on the quality of glass-ceramic wasteforms for plutonium immobilisation, consolidated by hot isostatic pressing. *J. Nucl. Mater.*, 485, 253–261.

Trachenko, K. (2004). Understanding resistance to amorphization by radiation damage. *J. Phys. Cond. Matt.*, 16, article no. R1491.

Trachenko, K., Pruneda, J. M., Artacho, E., and Dove, M. T. (2005). How the nature of the chemical bond governs resistance to amorphization by radiation damage. *Phys. Rev. B*, 71, article no. 184104.

Tracy, C. L., Park, S., Plevaka, M., and Bogdanova, E. (2021). Opportunities for US–Russian collaboration on the safe disposal of nuclear waste. *Bull. Atomic Sci.*, 77, 146–152.

Tumurugoti, P., Sundaram, S. K., Misture, S. T., Marra, J. C., and Amoroso, J. (2016). Crystallization behavior during melt-processing of ceramic waste forms. *J. Nucl. Mater.*, 473, 178–188.

Ueda, N., Vernerová, M., Kloužek, J., Ferkl, P., Hrma, P., Yano, T., and Pokorný, R. (2021). Conversion kinetics of container glass batch melting. *J. Am. Ceram. Soc.*, 104, 34–44.

Uruga, K., Tsukada, T., and Usami, T. (2020). Generation mechanism and prevention method of secondary molybdate phase during vitrification of PUREX wastes in liquid-fed ceramic melter. *J. Nucl. Sci. Techn.*, 57, 433–443.

Usami, T., Uruga, K., Tsukada, T., Miura, Y., Kiomamine, S., and Ochi, E. (2013). Proper-

ties of crystalline phase in waste glass. In *GLOBAL 2013: International Nuclear Fuel Cycle Conference – Nuclear Energy at a Crossroads, Salt Lake City*, Salt Lake City, USA.

Vance, E. R. (1994). Synroc: A suitable waste form for actinides. *MRS Bull.*, 19, 28–32.

Vance, E. R., Chavara, D. T., and Gregg, D. J. (2017). Synroc development—Past and present applications. *MRS Energy Sustain.*, 4, article no. E8.

Vance, E. R., Davis, J., Olufson, K., Chironi, I., Karatchevtseva, I., and Farnan, I. (2012). Candidate waste forms for immobilisation of waste chloride salt from pyroprocessing of spent nuclear fuel. *J. Nucl. Mater.*, 420, 396–404.

Vance, E. R., Moricca, S., Begg, B. D., Stewart, M. W. A., Zhang, Y., and Carter, M. L. (2010). Advantages hot isostatically pressed ceramic and glass-ceramic waste forms bring to the immobilization of challenging intermediate- and high-level nuclear wastes. *Adv. Sci. Technol. (Stafa-Zuerich, Switz.)*, 73, 130–135.

Vance, E. R., Stewart, M. W. A., and Moricca, S. (2014). Progress at ANSTO on SYNROC. *J. Austr. Ceram. Soc.*, 50, 38–48.

Vernaz, É. and Bruezière, J. (2014). History of nuclear waste glass in France. *Proc. Mater. Sci.*, 7, 3–9.

Vernaz, E., Veyer, C., and Gin, S. (2016). 6.15 – waste glasses. In Konings, R. J. M. and Stoller, R. E., editors, *Comprehensive Nuclear Materials*, pages 414–444. Elsevier, Oxford, 2nd edition.

Vienna, J., Piepel, G., Musick, C., Muller, I., and Pegg, I. (2006). Preliminary control strategy for hanford low-activity waste glass formulation. *Ceram. Trans.*, 176, 239–245.

Vienna, J. D. (2010). Nuclear waste vitrification in the United States: Recent developments and future options. *Int. J. Appl. Glass Sci.*, 1, 309–321.

Vienna, J. D. (2021). LAW additives and their utility. Personal communication.

Vienna, J. D., Hrma, P., Buchmiller, W. C., and Ricklefs, J. S. (2004). *Preliminary Investigations of Sulfur Loading in Hanford LAW Glass. PNNL-14649*. Pacific Northwest National Laboratory, Richland, WA, USA.

Vienna, J. D., Hrma, P., Crum, J. V., and Mika, M. (2001). Liquidus temperature–composition model for multi-component glasses in the Fe, Cr, Ni, and Mn spinel primary phase field. *J. Non-Cryst. Solids*, 292, 1–24.

Vienna, J. D., Kim, D. S., Muller, I. S., Piepel, G. F., and Kruger, A. A. (2014). Toward understanding the effect of low-activity waste glass composition on sulfur solubility. *J. Am. Ceram. Soc.*, 97, 3135–3142.

Walling, S. A., Gardner, L. J., and Hyatt, N. C. (2021a). ILW conditioning and performance. In Greenspan, E., editor, *Encyclopedia of Nuclear Energy*, pages 548–563. Elsevier, Oxford.

Walling, S. A., Kauffmann, M. N., Gardner, L. J., Bailey, D. J., Stennett, M. C., Corkhill, C. L., and Hyatt, N. C. (2021b). Characterisation and disposability assessment of multi-waste stream in-container vitrified products for higher activity radioactive waste. *J. Hazard. Mater.*, 401, article no. 123764.

Wang, F., Liao, Q., Dai, Y., and Zhu, H. (2016). Immobilization of gadolinium in iron borophosphate glasses and iron borophosphate based glass-ceramics: Implications for the immobilization of plutonium(III). *J. Nucl. Mater.*, 477, 50–58.

Wang, F., Liu, J., Wang, Y., Liao, Q., Zhu, H., Li, L., and Zhu, Y. (2020a). Synthesis and characterization of iron phosphate based glass-ceramics containing sodium zirconium phosphate phase for nuclear waste immobilization. *J. Nucl. Mater.*, 531, article no. 151988.

Wang, F., Lu, M., Liao, Q., Wang, Y., Zhu, H., Xiang, G., Li, L., and Zhu, Y. (2020b). Titanium-doped iron phosphate based glass ceramic waste forms containing 50 wt% simulated nuclear waste. *Mater. Chem. Phys.*, 239, article no. 122314.

Wang, F., Wang, Y., Liao, Q., Zhang, J., Zhao, W., Yuan, Y., Zhu, H., Li, L., and Zhu, Y. (2020c). Immobilization of a simulated HLW in phosphate based glasses/glass-ceramics by melt-quenching process. *J. Non-Cryst. Solids*, 545, article no. 120246.

Wang, G., Um, W., Kim, D.-S., and Kruger, A. A. (2019). 99Tc immobilization from off-gas waste streams using nickel-doped iron spinel. *J. Hazard. Mater.*, 364, 69–77.

Weber, W. J. (1990). Radiation-induced defects and amorphization in zircon. *J. Mater. Res.*, 5, 2687–2697.

Weber, W. J., Ewing, R. C., Catlow, C. R. A., de la Rubia, T. D., Hobbs, L. W., Kinoshita, C., Matzke, H., Motta, A. T., Nastasi, M., Salje, E. K. H., Vance, E. R., and Zinkle, S. J. (1998). Radiation effects in crystalline ceramics for the immobilization of high-level nuclear waste and plutonium. *J. Mater. Res.*, 13, 1434–

1484.

Weber, W. J., Ewing, R. C., and Meldrum, A. (1997). The kinetics of alpha-decay-induced amorphization in zircon and apatite containing weapons-grade plutonium or other actinides. *J. Nucl. Mater.*, 250, 147–155.

Wei, T., Zhang, Y., Kong, L., Kim, Y. J., Xu, A., Karatchevtseva, I., Scales, N., and Gregg, D. J. (2019). Hot isostatically pressed $Y_2Ti_2O_7$ and $Gd_2Ti_2O_7$ pyrochlore glass-ceramics as potential waste forms for actinide immobilization. *J. Eur. Ceram. Soc.*, 39, 1546–1554.

Wisniewski, W., Thieme, K., and Rüssel, C. (2018). Fresnoite glass-ceramics – A review. *Prog. Mater. Sci.*, 98, 68–107.

Wu, K., Wang, F., Liao, Q., Zhu, H., Liu, D., and Zhu, Y. (2020). Synthesis of pyrochlore-borosilicate glass-ceramics for immobilization of high-level nuclear waste. *Ceram. Int.*, 46, 6085–6094.

Wu, L., Li, H., Wang, X., Xiao, J., Teng, Y., and Li, Y. (2016a). Effects of Nd content on structure and chemical durability of zirconolite–barium borosilicate glass-ceramics. *J. Am. Ceram. Soc.*, 99, 4093–4099.

Wu, L., Wang, X., Li, H., Teng, Y., and Peng, L. (2016b). The effects of sulfate content on crystalline phase, microstructure, and chemical durability of zirconolite–barium borosilicate glass-ceramics. *J. Nucl. Mater.*, 478, 303–309.

Wu, L., Xiao, J., Wang, X., Teng, Y., Li, Y., and Liao, Q. (2018). Crystalline phase, microstructure, and aqueous stability of zirconolite–barium borosilicate glass-ceramics for immobilization of simulated sulfate bearing high-level liquid waste. *J. Nucl. Mater.*, 498, 241–248.

Xu, H., Wang, Y., Zhao, P., Bourcier, W. L., Van Konynenburg, R., and Shaw, H. F. (2004). Investigation of pyrochlore-based U-bearing ceramic nuclear waste: Uranium leaching test and TEM observation. *Env. Sci. Technol.*, 38, 1480–1486.

Xu, H., Wu, L., Zhu, J., and Navrotsky, A. (2015a). Synthesis, characterization and thermochemistry of Cs-, Rb- and Sr-substituted barium aluminium titanate hollandites. *J. Nucl. Mater.*, 459, 70–76.

Xu, K., Pierce, D. A., Hrma, P., Schweiger, M. J., and Kruger, A. A. (2015b). Rhenium volatilization in waste glasses. *J. Nucl. Mater.*, 464, 382–388.

Xu, X., Youngman, R. E., Kapoor, S., and Goel, A. (2021). Structural drivers controlling sulfur solubility in alkali aluminoborosilicate glasses. *J. Am. Ceram. Soc.*, 104, 5030–5049.

Yang, Y., Cao, X., Shi, L., Zhang, Z., Wang, P., Li, J., Sun, Y., Chen, S., Wang, T., Ma, L., and Peng, S. (2021). Thermal evolution effects on the properties of converting Cs-polluted soil into pollucite-base glass-ceramics for radioactive cesium immobilization. *J. Materiomics*, 7(6), 1335–1343.

Yoshioka, M., Torata, S., Igarashi, J., Takahashi, T., and Horie, M. (1992). Glass melter and process development for PNC Tokai vitrification facility. *Waste Manag.*, 12, 7–16.

Yudintsev, S. V., Stefanovsky, S. V., Nikonov, B. S., Stefanovsky, O. I., Nickolsky, M. S., and Skvortsov, M. V. (2019). Phase formation at synthesis of murataite-crichtonite ceramics. *J. Nucl. Mater.*, 517, 371–379.

Zhang, Y., Gregg, D. J., Kong, L., Jovanovich, M., and Triani, G. (2017a). Zirconolite glass-ceramics for plutonium immobilization: The effects of processing redox conditions on charge compensation and durability. *J. Nucl. Mater.*, 490, 238–241.

Zhang, Y., Karatchevtseva, I., Kong, L., Wei, T., and Zhang, Z. (2018). Structural and spectroscopic investigations on the crystallization of uranium brannerite phases in glass. *J. Am. Ceram. Soc.*, 101, 5219–5228.

Zhang, Y., Kong, L., Aughterson, R. D., Karatchevtseva, I., and Zheng, R. (2017b). Phase evolution from $Ln_2Ti_2O_7$ (Ln = Y and Gd) pyrochlores to brannerites in glass with uranium incorporation. *J. Am. Ceram. Soc.*, 100, 5335–5346.

Zhang, Y., Wei, T., Zhang, Z., Kong, L., Dayal, P., and Gregg, D. J. (2019). Uranium brannerite with Tb(III)/Dy(III) ions: Phase formation, structures, and crystallizations in glass. *J. Am. Ceram. Soc.*, 102, 7699–7709.

Zhang, Y., Zhang, Z., Thorogood, G., and Vance, E. R. (2013). Pyrochlore based glass-ceramics for the immobilization of actinide-rich nuclear wastes: From concept to reality. *J. Nucl. Mater.*, 432, 545–547.

Zhang, Z., Spiers, K. M., Vance, E. R., and Davis, J. (2020). Partitioning of Ce, as a simulant for Pu, in a multi-phase ceramic nuclear waste form. *J. Am. Ceram. Soc.*, 103, 5515–5524.

Zhao, D., Li, L., Davis, L. L., Weber, W. J., and Ewing, R. C. (2001). Gadolinium borosilicate glass bonded Gd-silicate apatite: a glass-ceramic nuclear waste form for actinides. *Mat. Res. Soc. Symp. Proc.*, 663, 199–206.

Zhou, S., Liu, X., Qian, Z., Qiao, Y., Yu, B., Li, L., Wang, S., and Qin, Q. (2021). Preparation and characterization of phosphate glass–ceramic wasteform with strontium fluoride. *J. Radioan. Nucl. Chem.*, 328, 217–224.

Zhu, H., Wang, F., Liao, Q., and Zhu, Y. (2020). Synthesis and characterization of zirconolite-sodium borosilicate glass-ceramics for nuclear waste immobilization. *J. Nucl. Mater.*, 532, article no. 152026.